

AN INTERCOMPARISON OF FIVE AMMONIA MEASUREMENT TECHNIQUES

E. J. Williams^{1,2}, S. T. Sandholm³, J. D. Bradshaw³, J. S. Schendel³, A. O. Langford^{1,2},
 P. K. Quinn^{1,2,7}, P. J. LeBel⁴, S. A. Vay⁴, P. D. Roberts^{5,8}, R. B. Norton¹, B. A. Watkins^{1,2},
 M. P. Buhr^{1,2}, D. D. Parrish¹, J. G. Calvert⁶, and F. C. Fehsenfeld^{1,2}

Abstract. An intercomparison has been conducted among five instruments which measure gas phase ammonia at low concentration in the atmosphere: (1) a photofragmentation/laser-induced fluorescence (PF/LIF) instrument; (2) a molybdenum oxide annular denuder sampling/chemiluminescence detection (MOADS) technique; (3) a tungsten oxide denuder sampling/chemiluminescence detection (DARE) system; (4) a citric acid coated denuder sampling/ion chromatographic analysis (CAD/IC) method; and (5) an oxalic acid coated filter pack sampling/colorimetric analysis (FP/COL) method. Mixtures of ammonia in air at flow rates of 1800 (STP) L/min and concentrations from 0.1 to 14 parts per billion by volume (ppbv) with the addition of possible interferants (CH_3NH_2 , CH_3CN , NO , NO_2 , O_3 , and H_2O) were provided for simultaneous tests. In addition, the five instruments made simultaneous ambient air measurements both from a common manifold and from their separate inlets located at a common height above the ground. Several conclusions were reached: (1) No artifacts or interferences were conclusively established for any of the techniques, although CH_3NH_2 may interfere in the MOADS system. (2) Measurements from the PF/LIF and the CAD/IC methods agreed well with the prepared mixtures over the full range of ammonia concentrations. The high specificity and time resolution (1 min) of the PF/LIF results allowed data from this technique to be used as a basis set for comparisons. (3) For fog-free conditions, ambient measurements from all of the instruments generally agreed to within a factor of 2 for ammonia levels above 0.5 ppbv. The CAD/IC and PF/LIF instruments agreed to within 15% on average for all ambient data. (4) The slope from linear regression analysis of separate inlet ambient air measurements indicated that the DARE data agreed with those from the PF/LIF system to within 7%. The linear regression line intercept was 216 parts per trillion by volume (pptv), which may indicate a positive interference in the DARE data, but the DARE data were closer to the PF/LIF data (50 - 100 pptv higher) at the lowest ambient ammonia levels. (5) The FP/COL method measured about 66% of the ammonia as determined by the PF/LIF technique and measured even lower fractional levels in the prepared samples. These low values indicate a loss of ammonia, possibly on the Teflon prefilter, under the conditions of this study (cold temperatures

and generally low relative humidity). (6) The MOADS ambient air data were about 64% of the ammonia that was observed by the PF/LIF method for levels greater than about 1 ppbv, and below this level it overestimated ammonia. Problems with the MOADS calibrations and inlets may have been responsible. (7) Ambient air data from the one period of fog formation indicated that ambient ammonia was primarily partitioned into the condensed phase, leaving the interstitial air greatly depleted. Volatilization of absorbed ammonia from water droplets entrained in the sampled air appeared to influence the MOADS system. This did not appear to affect the FP/COL, CAD/IC, or PF/LIF results as a result of fast sample flows and/or operation at ambient temperatures.

1. Introduction

Ammonia is an important trace species in the troposphere. It rapidly associates with acids in the atmosphere and thus plays an important role in aerosol formation. Incorporation of NH_3 into aerosols and cloud water can strongly influence the pH, which is a controlling factor in condensed phase chemical reactions [Seinfeld, 1986]. Under some conditions, ammonia may be a photochemical source or a sink of NO_x , depending on the concentrations of NO_x and O_3 present; but these pathways are usually negligible because of the long lifetime of NH_3 with respect to OH attack [Warneck, 1988].

Most atmospheric NH_3 is derived from biogenic sources [National Research Center (NRC), 1979]. A majority of this ammonia is produced by the biogenic decomposition of organic materials and from animal excrement. Another major source is fertilizer production and use. Ammonia is involved in plant metabolism and can be exchanged (emitted or absorbed) between vegetation and the atmosphere [Fahrquar et al., 1983]. Ammonia also can be directly volatilized by burning biomass [LeBel et al., 1991; Lobert et al., 1990].

Presently, the knowledge of the sources and sinks of ammonia and its trends, distribution, and chemistry in the atmosphere is limited by the availability of reliable techniques which are capable of determining NH_3 in real time at low abundances (<1 part per billion by volume (ppbv)). Considerable effort has been expended to develop this technology, and new methods are emerging. For this reason it is important to establish unambiguously the capabilities of the techniques and the comparability of the data sets obtained by them. Intercomparisons of gaseous ammonia measurement techniques have been carried out previously [Appel et al., 1988; Fern et al., 1988; Gras, 1984; Harrison and Kitto, 1990; Sickles et al., 1988; Wiebe et al., 1990]. These experiments relied on the results of field measurements to ascertain the comparability of the tested methods. The instrument intercomparison reported here not only involved field measurements but also included evaluation of the tested methods for response to ammonia and other species under controlled conditions as well as an intercomparison of ammonia standards. The five methods included photofragmentation/laser-induced fluorescence, molybdenum oxide annular denuder sampling with chemiluminescence detection, tungsten oxide denuder sampling with chemiluminescence detection, citric acid coated denuder sampling with ion chromatographic analysis, and oxalic acid coated filter pack sampling with colorimetric analysis. The goal of this study was to assess, via intercomparison, the reliability with which ammonia can be measured in the boundary layer by these techniques.

¹Aeronomy Laboratory, National Oceanic and Atmospheric Administration, Boulder, Colorado.

²Cooperative Institute for Research in Environmental Sciences, University of Colorado, Boulder.

³School of Earth and Atmospheric Sciences, Georgia Institute of Technology, Atlanta.

⁴Langley Research Center, National Aeronautics and Space Administration, Hampton, Virginia.

⁵Hampton University, Hampton, Virginia.

⁶National Center for Atmospheric Research, Boulder, Colorado.

⁷Currently at Pacific Marine Environmental Laboratory, National Oceanic and Atmospheric Administration, Seattle, Washington.

⁸Currently at College of William and Mary, Williamsburg, Virginia.

Copyright 1992 by the American Geophysical Union.

Paper number 92JD00721.
 0148-0227/92/92JD-00721\$05.00

The intercomparison involved three stages. First, spike tests in filtered ambient air or zero air were conducted to test instrument responses both to ammonia and to possible interferant species. The protocol for these tests was single blind in that the investigators were not aware of the type of spike gas nor the level at which it was added to the sampled gas stream. Ammonia, methylamine (CH_3NH_2), acetonitrile (CH_3CN), the oxides of nitrogen ($\text{NO} + \text{NO}_2 = \text{NO}_x$), O_3 , and water vapor were the compounds used for these standard addition tests. Second, a period of ambient air sampling from a common manifold was carried out. This procedure was used to minimize differences among the data sets that could be attributable to ambient variability. Third, a period of ambient air sampling was conducted during which the instrument inlets were placed at a common height (5 m) above the ground. This sampling period was undertaken to compare how each group would independently characterize the ambient levels of ammonia at the site. This paper describes the instruments used, the testing protocols employed, and the results from the intercomparison. The most definitive results were from the ambient sampling, and these will be emphasized in the discussion. Interpretation of the spike tests is hampered principally by changing background levels of ammonia but also by uncertainty in the supplied test mixtures of trace species. However, the spike tests demonstrated that at least some of the techniques measured ammonia accurately, provided useful upper limits on potential interferences, and provided insight into the causes of differences observed in the ambient sampling results.

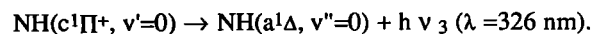
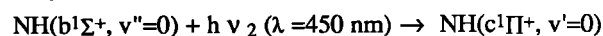
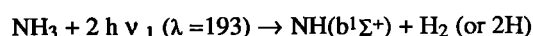
2. Experiment

2.1. Measurement Site

The intercomparison was conducted from February 27 to March 28, 1989, at Green Mountain Mesa, which is about 3 km to the south of downtown Boulder, Colorado, at an elevation of approximately 1770 m. At this site the ammonia levels can vary substantially. High levels of 1 ppbv to >10 ppbv are associated with regional agricultural activities to the east and north of Boulder. Air parcels transported to the site from this area can be quite polluted with relatively high levels of a variety of trace compounds of anthropogenic origin. Conversely, much lower levels of ammonia (<100 parts per trillion by volume (pptv)) can be observed when the wind is from the west where there are no substantial sources of ammonia for hundreds of kilometers.

2.2. Measurement Techniques

2.2.1. Vacuum UV photofragmentation/laser-induced fluorescence (Georgia Institute of Technology). The photofragmentation/laser-induced fluorescence (PF/LIF) technique uses a near-vacuum UV ArF excimer laser ($\lambda = 193$ nm) to photolyze NH_3 via a two-photon process, thereby producing a NH photofragment with significant yield in the long-lived metastable electronic state, $\text{NH}(\text{b}^1\Sigma^+)$. Within microseconds the prompt luminescence background generated by the 193-nm photolysis laser will decay by several orders of magnitude. After a short delay time (2–10 μs) a second probe laser ($\lambda = 450$ nm) is then used to interrogate the $\text{NH}(\text{b}^1\Sigma^+)$ state population via excitation of a specific rotationally resolved transition. The resultant fluorescence is then observed in a spectral window, near 326 nm, that is capable of resolving the vibrational structure of the fluorescing transition. The spectral and temporal selectivity of this true photofragmentation/LIF method permits significantly greater detection sensitivity and selectivity than simpler photofragmentation/prompt luminescence techniques. The PF/LIF NH_3 detection scheme can be summarized by



The basic detection hardware configuration of the prototype instrument deployed in this intercomparison has been previously described [Schendel et al., 1990; van Dijk et al., 1989], and only a brief summary of the salient features and operating parameters specific to this intercomparison is given here.

The sampling manifold and calibration flow loops were constructed entirely of glass or passivated nickel, which both exhibit minimal adsorption-related memory effects. In order to further reduce these effects as well as to minimize aerosol decomposition the ambient flow manifold and fluorescence sampling cell were designed for operation under a high flow rate near ambient pressure conditions (using > 5.0 cm ID tubing). The long ambient sampling manifold used in this intercomparison was approximately the same length as that utilized for connection to the referee's common manifold system (i.e., approximately 7.5 m). Flow rates ranging from 300 to 2500 (STP) L/min were used during this intercomparison. These high flow rates yielded sample residence times ranging from 2.3 s to < 0.3 s, respectively (with 1–25 mbar total pressure drop). The sample manifold was also wrapped with heating tape and thermal insulation. During normal ambient sampling periods the flow line was maintained near outside air temperature (i.e., $\leq 2.5^\circ\text{C}$ temperature differential). In order to minimize aerosol decomposition, heat was only applied to the sample manifold in order to clean the flow line or to perform other types of sampling tests.

Calibration of the instrument was accomplished in a three-tier manner. Data normalization, using the signal measured from a reference cell containing a known mixture of NH_3 and nitrogen, constitutes the first tier, which is instrumentally equivalent to an internal standard. The second tier involved calibrations using isotopic $^{15}\text{NH}_3$ as a working gas standard. The spectroscopic selectivity of the PF/LIF approach makes possible the resolution of the $^{15}\text{NH}(\text{b}^1\Sigma^+, v''=0) \rightarrow ^{15}\text{NH}(\text{c}^1\Pi^+, v'=0)$ transitions from their ^{14}NH counterparts (separated by 1.5 cm^{-1}). Under conditions of high ambient variability the use of isotopic $^{15}\text{NH}_3$ has made possible standard addition calibrations and isotope dilution tests at concentrations near those of the ambient $^{14}\text{NH}_3$ levels. This procedure improves the precision of calibrations due to the very low level of $^{15}\text{NH}_3$ in the atmosphere. The third calibration tier involved direct calibration of the system by the method of standard addition using a primary $^{14}\text{NH}_3$ certified gas standard. The calibration flow system was based on a three-stage continuous (dynamic) serial dilution system. All flows were measured using mass flow meters that were cross checked against volume displacement standards. Calibration gas was supplied from certified 100 parts per million by volume (ppmv) NH_3 (in nitrogen) primary standard cylinders. Direct injection of the diluted gas standard occurred near the inlet of the sampling manifold through a continuously flowing preequilibrated calibration flow loop. The calibration system could provide standard addition ranging from 200 pptv to 20 ppbv for either $^{15}\text{NH}_3$ or $^{14}\text{NH}_3$.

Correction of the measured ambient signal for the effect of water vapor collisional deactivation of the $\text{NH}(\text{b}^1\Sigma^+)$ metastable state population is now a well-understood process [Van Dijk et al., 1989] and depends only on the measurement of the absolute concentration of water vapor and the time delay between the photolysis and probe laser pulses. Under less than favorable conditions, where the water vapor that is observed at the calibration point differs by 13 mbar from that of the ambient measurement, the normalization factor accounting for water quenching will have an accuracy of $\pm 10\%$ (1 σ)

for the nominal probe laser delay times used during the intercomparison (e.g., $2 \mu\text{s} < \Delta t < 8 \mu\text{s}$). All data measurements taken during this intercomparison were normalized using water vapor measurements obtained with a General Eastern two-stage dew point hydrometer.

The PF/LIF system was tested for a number of potential interferences prior to this intercomparison program [Schendel et al., 1990]. Tests carried out on NH_2CH_3 , $\text{NH}(\text{CH}_3)_2$, $\text{N}(\text{CH}_3)_3$, and $\text{NH}_2\text{C}_2\text{H}_5$ showed no significant interference (i.e., $< 10\%$) for equal concentrations of NH_3 and RNH_x . Interferences associated with the thermal decomposition of aerosols were minimized, to the extent possible, by utilization of short sample residence times at near-ambient temperatures and pressure. Memory effects were not seen when sampling ambient air based on manifold cleaning exercises that were carried out under relatively stable air mass conditions and on tenfold variations in sample flow rate (i.e., residence time).

The PF/LIF instrument used in this intercomparison demonstrated a limit of detection ($S/N = 2/1$) of < 5 pptv ($< 0.2 \text{ nmol/m}^3$) for a measurement integration period of 5 min. While the PF/LIF method is inherently linear over 5 orders of magnitude, the linear dynamic range of this particular instrument was limited to 40 dB increments by the dynamic range of the particular gated photon counting system employed (i.e., signal attenuation was necessary for approximately every 100-fold increase in NH_3 concentration above the LOD). Absolute accuracy of the measurement is estimated to be $\pm 18\%$ at the 95% confidence limit. Relative measurement precision was typically $\pm 15\%$ (1σ), for an ambient NH_3 concentration of 100 pptv and an instrument integration time of 1 min.

2.2.2. Molybdenum oxide annular denuder system (Aeronomy Laboratory, NOAA). The molybdenum oxide annular denuder system (MOADS) is described in detail elsewhere [Langford et al., 1989], and the following section will be concerned primarily with changes from the published configuration and details of the calibration and sampling procedure unique to the intercomparison. Each denuder consists of an oxidized molybdenum rod supported in a quartz tube (maintained at 50°C) through which air is sampled at a rate of $\sim 1 \text{ L/min}$ for a period of 30 min. The tube is then heated to 400°C in a flow of nitrogen to desorb the collected NH_3 and any other adsorbed species. Speciation is based on desorption temperature and only the alkylamines ($(\text{C}_n\text{H}_{2n+1})_x\text{NH}_{3-x}$) cannot be distinguished from NH_3 . Part of the collected NH_3 is oxidized to NO in the desorption process and this fraction analyzed using a standard NO- O_3 chemiluminescence detector. Nitric oxide calibration gas (traceable to a standard certified by the National Institute for Standards and Technology, formerly the National Bureau of Standards) is injected into the carrier stream as an internal standard for 4 min near the end of each desorption cycle to correct for drift in the chemiluminescence detector response. The ratio of each NH_3 desorption peak to the corresponding internal standard peak is compared to archived calibration curves to quantify NH_3 . Two denuders are used to obtain a continuous record and are mounted in individual enclosures that can be separated by as much as 12 m for gradient measurements. Commercial chromatography software (Dynamic Solutions, Milford, Massachusetts) is used for data analysis and the system is fully automated to operate for up to 7 days without user intervention.

The system is calibrated by introducing a small flow ($\leq 50 \text{ STP cm}^3/\text{min}$) of NH_3 in zero air through a tee manually attached to the denuder inlets. The latter consist of 0.635 cm ID TFE tees and are maintained at 50°C during sampling. The primary standard is a gravimetrically calibrated wafer-type permeation device (VICI Metronics, Santa Clara, California) maintained at 30°C and continuously bathed in zero air ($50 \text{ cm}^3/\text{min}$) that flows through a 15-m loop of 0.32 cm PFA tubing from the source to the sampling inlets on the trailer

roof. The loop is physically broken at a union near the samplers and attached to the inlets during calibration. A second, much larger flow of zero air is added below the calibration tee to exclude ambient air. Calibration points are obtained by changing the NH_3 concentration in the flow or by changing the length of time the spike is injected. For reasons described below, only the latter approach was used during the intercomparison. These approaches are equivalent since the instrument actually measures the total mass (in nanograms) of adsorbed NH_3 , and this is normally converted to atmospheric mixing ratios (pptv @STP) using the known volume of sampled air. Calibration curves of 8–10 points are generated and used to calculate the loading and mixing ratio for each ambient sample. The response becomes nonlinear above $\sim 40 \text{ ng NH}_3$ ($\sim 2 \text{ ppbv}$ in 0.9 L/min) and the curves are fit as a third-order polynomial. The response is checked every few days and new calibration curves generated when drift becomes apparent. A separate response curve is determined for each denuder.

Several problems arose during the course of the intercomparison that limited the performance of the system. During the manifold tests the NH_3 levels in the calibration loop changed slowly ($\pm 20\%$) over the course of the 6–8 hours required to generate the calibration curves. This was attributed to changes in the amount of NH_3 adsorbed on the walls of the unheated calibration loop with ambient temperature. A second loop heated to 30°C was installed during the last week of the intercomparison to circumvent these problems. In addition, the dilution system used to change the NH_3 concentration in the calibration stream did not work and the lowest calibration point that could be obtained was ~ 500 pptv. Thus it was necessary to extrapolate below this value (normally, the calibration curve extends to ~ 50 pptv). Such extrapolation is dangerous when the system is exposed to high ($> 5 \text{ ppbv}$) mixing ratios (as is often the case in Boulder) since these lead to background levels or memory effects due to NH_3 desorption from the inlets. An upper limit for this effect was estimated by exposing the denuders to 701 ng of NH_3 in $100 \text{ cm}^3/\text{min}$ zero air ($\sim 32.0 \text{ ppbv}$ in a 0.9 L/min sample flow) for one sample period and then sampling clean zero air for the next 10 cycles. The second cycle showed a residual of 4.4 ng (0.20 ppbv in a 0.9 L/min sample flow) indicating that $\geq 99.6\%$ of the adsorbed NH_3 was desorbed in 1 cycle. After five more cycles, the residual had decreased to 0.8 ng (40 pptv in a 0.9 L/min sample flow) and after 10 cycles the residual remained at 0.6 ng , equivalent to 30 pptv in a 0.9 L/min sample flow. Thus signal levels of 0.1 to 0.2 ppbv can be observed for several hours after the ambient mixing ratios decrease from $\geq 5 \text{ ppbv}$ to $\leq 0.5 \text{ ppbv}$. Variability of this magnitude was often encountered during the ambient sampling periods of the intercomparison and is likely responsible for the higher mixing ratios observed by MOADS on several occasions. It is important to note that at other sites (e.g., Niwot Ridge), where the denuders are rarely exposed to mixing ratios above $\sim 1 \text{ ppbv}$, this residual will remain near $\sim 30 \text{ pptv}$ and can safely be neglected.

For the manifold tests the samplers were attached by bolting the bottoms of the aluminum enclosures directly onto the pyrex tees. A thin sheet of PFA film isolated the aluminum surfaces from the manifold. Although this configuration probably created a dead volume between the main flow in the manifold and the MOADS inlets, this approach was chosen to duplicate the normal sampling conditions as closely as possible. In particular, it was deemed undesirable to introduce a sampling line between the MOADS inlets and the manifold in view of the small sampling flow ($\sim 1 \text{ L/min}$). Since the inlets were inaccessible for calibration purposes, this was done by introducing the NH_3 standard through the inlet tee.

2.2.3. Tungsten oxide denuder atmospheric research experiment (DARE) (Langley Research Center, NASA).

The tungsten oxide denuder consists of a 6-mm OD quartz tube with the interior surface coated by vacuum deposition of tungsten oxide (WO_3). The technique, described by Braman et al. [1982, 1986] and LeBel et al. [1985], involves collection of a sample by passing air through the denuder at a flow rate of 1 L/min. Ammonia and nitric acid in the air sample are chemisorbed on the WO_3 surface. After sample collection the denuder is heated to 350°C with carrier gas flowing and the collected NH_3 and HNO_3 are desorbed. Nitric acid is desorbed as NO and detected by a chemiluminescence detector, while ammonia is desorbed as NH_3 and is recollected on a WO_3 -coated transfer tube. The transfer tube is then heated to 350°C; collected NH_3 desorbs, is converted to NO catalytically over a gold surface at 650°C, and is detected by chemiluminescent reaction of NO with ozone. The integrated desorption curve, with baseline subtracted, is related to the NH_3 concentration in the air sample by calibration. Measurements from aircraft indicate that the DARE system is probably not affected by variations in temperature and relative humidity encountered during flights (P. J. LeBel et al., unpublished manuscript, 1989). In addition, denuder tube lifetime problems experienced by others [Roberts et al., 1988; Langford et al., 1989] have not been observed with the DARE WO_3 tube coatings.

The DARE instrument configuration for the NH_3 intercomparison is similar to the system designed for measurements from aircraft for background tropospheric applications [LeBel et al., 1985, 1990] and for biomass-burning applications [LeBel et al., 1991]. A small computer controls data acquisition, analysis and system control functions. Data are stored on a magnetic disk for later retrieval, if needed. Sampling time is variable from a fraction of a minute to hours. A sample is analyzed immediately after collection; sample analysis time is approximately 7 min. Because the system is automated, repetitive and unattended measurements can be made. The NO detection system is a sensitive chemiluminescence system [Torres, 1985] designed especially for measurements from aircraft in the background troposphere. The DARE denuder system has an NH_3 detection limit of approximately 40 pptv for a 10-min sample with an accuracy of 15 to 20% and a precision of about 10%.

During the NH_3 intercomparison the DARE denuder system was calibrated periodically using a permeation wafer NH_3 source (Vici Metronics, Santa Clara, California) maintained at 30°C in a temperature-controlled chamber. The chamber has battery backup power to maintain temperature in the event of power failure. The source output is monitored by regular gravimetric measurements. Zero air carrier gas at 50 cm^3/min flows continually over the permeation wafer. During calibration the carrier flow containing NH_3 from the permeation source is diluted with zero air (UZAM grade, Scott Specialty Gases, San Bernadino, California). The dilution flow is adjusted to give the desired NH_3 concentration and is maintained for sufficient time for transfer lines and sampling manifold to equilibrate prior to calibration.

In setting up the DARE experiment for this intercomparison, there was concern that the high winds that occur at this site in winter might break the 25-mm all-glass transfer line which connected the instrument inlet in one trailer to the common sampling manifold which was mounted on the roof of a different trailer. For this reason, a 0.91-m section of flexible stainless steel tubing lined with 22-mm ID TFE Teflon was installed in the transfer line. This flexible section was in place for all common manifold experiments. The use of a material other than glass, the preferred choice, may have contributed to problems encountered during common manifold sampling (see section 3). For ambient sampling the entire DARE transfer line consisted of a 25-mm ID glass with an inverted funnel-shaped inlet to prevent water droplets from being sucked into the transfer line. For each configuration the

transfer line was about 5.5 m in length. This is 1.5 times longer than the normal ground-based sampling configuration and nearly 5 times longer than the typical aircraft inlet configuration. A manifold flow rate of 200 L/min was maintained throughout the intercomparison with an average sample residence time of 0.7 s. The entire manifold and transfer line was wrapped with heat tape and insulation, but the heaters were not used during normal sampling conditions.

2.2.4. Citric acid denuder/ion chromatography (CAD/IC) (Aeronomy Laboratory, NOAA). Gaseous ammonia is collected by drawing air through a citric acid coated denuder tube. The denuder is a glass tube 62 cm long with an inside diameter of 6 mm. Airflow through the tube is maintained at a fixed rate of 2 L/min with a flow controller. The measured collection efficiency for this tube was 95%. However, the results reported in this paper were not corrected for this slightly less than 100% efficiency. Both the theoretical and measured collection efficiency for this tube is approximately 95%. Collected NH_3 is extracted as NH_4^+ from the tube with 5 ml of either deionized (DI) water or 5 mM hydrochloric acid (HCl) solution. The extract is then analyzed with a Dionex ion chromatograph equipped with an ion exchange cation column, micromembrane suppressor, and conductivity detector. The ammonium ion concentration in the sample is determined by normalization to an ammonium standard. These standards are made by dilution of 1000 part per million by mass (ppmm, mg kg^{-1}) solution of NH_4^+ prepared from NH_4Cl . Given the ammonium ion concentration in the extract, the flow rate of air through the tube, and the sampling duration, the average atmospheric NH_3 concentration can be calculated. In concept this system is the same as that proposed and used by Ferm [Ferm, 1979; Ferm et al., 1988].

The detection limit of the chromatographic system for NH_4^+ is approximately 0.001 ppmm in solution. This leads to an equivalent atmospheric NH_3 mixing ratio of about 25 pptv for the operating parameters normally used (flow rate of 2 L/min and sample period of 2 hours). The detection limit of the overall system is somewhat larger and is usually determined by the variability of background NH_4^+ found in different denuder tubes. The average background in the tubes is 0.003 ± 0.002 (2) ppmm NH_4^+ , which is equivalent to an atmospheric NH_3 level of 75 ± 50 pptv. We are unaware of any compound that has the same retention time as the ammonium ion. Sodium, potassium, methylamine, and ethylamine have similar retention times to that of ammonium but are chromatographically resolved unless they are present in very large quantities. In principle, aerosols may cause some increase in apparent NH_3 concentration by impaction with the front end of the denuder tube and by evaporation of labile aerosol NH_4NO_3 with subsequent adsorption of NH_3 by the tube as aerosols travel through the denuder. Evidence for this effect from previous work [Langford et al., 1989] is inconclusive, however, and in any case, these are minor effects unless aerosol ammonium is large compared to gaseous ammonia. The denuder tubes were coupled to the common sampling manifold via a glass adaptor which positioned the inlet of the denuder tube directly in the main manifold flow. The adaptor was a tube into which the denuder was inserted. Glass dimples separated the denuder from the guide tube and a pump drew air (at about 6 L/min) from the manifold through the annulus between the tubes to prevent any stagnant air from being sampled.

2.2.5. Filter pack/colorimetry (FP/COL) (CIRES, University of Colorado). The filter pack method allows for the simultaneous collection of particle NH_4^+ and gaseous NH_3 . Since it is a preconcentration technique, it also allows for the sampling of NH_3 at very low concentrations. In this study the filter pack consisted of five filters in series. The first was a 47-mm Millipore Teflon filter (1.0 μm pore size) for the collection of particles. The remaining four were 47-mm Whatman 41

filters coated with 0.01 M oxalic acid for the collection of NH_3 . Four coated filters were used to increase the NH_3 collection efficiency in the case of breakthrough.

The Whatman filters were washed with 4 L of 1.2 M HCl followed by 4 L of deionized water. After washing, they were vacuum dried and stored frozen in acid-washed sealed petri dishes. One to 24 hours before use, the filters were placed in a NH_3 -free glove box and coated with 0.01 M oxalic acid. For the first 38 samples taken, the oxalic acid was prepared in a 16/84 (by volume) glycerol/methanol ("Photrex" reagent grade methanol) solution and for the last 21, in a 32/68 (by volume) glycerol/methanol solution. In both cases the filters were left to dry in the glove box. The coated filters were stored in acid-washed sealed petri dishes in the glove box until use. The 47-mm filter packs (Nuclepore Corporation, Pleasanton, California) used to hold the Teflon and Whatman filters were soaked for 2 to 4 hours in 1.2 M HCl and rinsed thoroughly with deionized water prior to use.

For manifold sampling, the top stage of the filter pack was fitted with a 0.95-cm (OD) threaded male connector. This was threaded to a 6.35-cm-long acetal tube which, in turn, was attached to the manifold through a 7.6-cm (ID) x 1.6-cm-long glass adaptor. The connecting tube was made of acetal as this material has been shown not to absorb detectable amounts of NH_3 at 75% RH and 22°C [Quinn and Bates, 1989]. A second filter pack was mounted with each sample to serve as a sampling and analytical field blank (average sample flow rate was 64.1 L/min while blank flow rate was 0 L/min). The manifold port for the filter pack system was constructed so that the sample and blank filter packs were mounted directly across from each other and were wrapped with foam insulation to prevent condensation of moisture from the warm manifold air. During ambient sampling the sample and blank filter packs were mounted side by side approximately 7.6 cm apart and 5 m above the ground.

After sample collection the filter packs were transferred to an NH_3 -free glove box. Once in the glove box, each oxalic acid coated filter was put into a centrifuge tube containing 10 mL of deionized water. The filter solution then was agitated ultrasonically for 30 min and centrifuged for 10 min. The aqueous extract was decanted into a vial. The samples were analyzed within 1 to 7 hours of collection by the phenolphthorite colorimetric technique [Harwood and Kuhn, 1970; Solarzano, 1969] using a Technicon autoanalyzer II (Technicon Corporation, Tarrytown, New York). This technique involves the reaction of ammonia with phenol and hypochlorite in the presence of a catalyst (sodium nitroprusside) to form a blue-colored indophenol moiety. The absorbance of the solution is monitored at 630 nm through a 5-cm pathlength cell. No N(III) species are known to interfere with the analysis [Solarzano, 1969]. A calibration curve was generated for each day of analysis by dilution of a 55.5 mM NH_4^+ (as NH_4Cl) stock standard to a series of five standards ranging from 0.5 to 22.2 μM NH_4^+ . Concentrations were calculated by fitting the calibration curve to a second-order polynomial function. When necessary, samples were diluted by a factor of 2 to 100 to correspond to the calibration curve range.

The collection efficiency of the method has been tested [Quinn and Bates, 1989] by passing a known amount of NH_3 through the filter pack. The NH_3 source was a gravimetrically calibrated permeation tube. On the basis of these tests the precision of the method is $\pm 39\%$ and the accuracy is $\pm 30\%$ at room temperature and 75% RH. The collection efficiency was found to depend on relative humidity. At 75% RH the NH_3 collection efficiency was $103 \pm 30\%$ with 92% of the ammonia collected by the first filter, 6% collected by the second filter, and 2% collected by the third. At 40% RH the collection efficiency was $33 \pm 28\%$. For this intercomparison no correction was made for the dependence of the collection

efficiency on relative humidity. It has also been suggested that NH_4^+ -containing particles could yield an artificially high NH_3 concentration as they may volatilize from the Teflon filter [Gras, 1984; Harrison and Kitto, 1990].

Errors propagated for individual samples in this study were based on the precision of the method, errors in the colorimetric analysis, and by comparison to a laboratory-measured collection efficiency of 92% at 75% RH for the first filter in the series. The detection limit of the method, defined as the concentration required to give a signal equal to twice the standard deviation of the blank, is 36 pptv for a 2-hour sample time and 1.8 pptv for a 36-hour sample time at a flow rate of 50 L/min.

2.2.6. Supporting measurements. During the ambient sampling portion of the intercomparison the following were also measured: NO (chemiluminescence); NO_2 (photolysis/chemiluminescence); PAN (GC-ECD); HNO_3 (filter pack); NO_y (gold catalytic converter/chemiluminescence) O_3 (UV absorption, model 1003, Dasibi Corporation, Glendale, California, and model 49, Thermo Electron Corporation, Hopkinton, Massachusetts); nitrate, sulfate, and ammonium in particulates (filter pack and ion chromatography); SO_2 (pulsed fluorescence, model 43S, Thermo Electron Corporation, Hopkinton, Massachusetts); CO (nondispersive infrared absorption, model 48, Thermo Electron Corporation, Hopkinton, Massachusetts); solar UV (radiometer, Eppley Corporation, Newport, Rhode Island); and meteorological parameters (temperature, dew point, pressure, wind speed, and wind direction).

2.3. Manifold Sampling System and Standards

Initially, the ammonia instruments were connected to a common sampling manifold shown schematically in Figure 1. This manifold system allowed simultaneous evaluation of the performance of all the ammonia detectors when sampling either artificially produced air samples or ambient air. Because of the high flow rates needed for the tests (nominally 1800 L/min) the manifold was constructed of a 7.6-cm ID Pyrex glass pipe (Corning conical process pipe system, Corning Glass Works, Corning, New York) connected with Teflon gaskets (3-mm thickness). The total length was about 8 m. The glass pipe was supported by a rigid framework that was mounted on the roof of one of the trailers. Instrument inlets were attached to the manifold by a series of tees (and one 4-way cross). Each investigator was responsible for the design and construction of an adaptor that mated his or her inlet to the manifold. The entire section of glass pipe that was exposed to the outside environment was wrapped with heating tape and insulation to keep the glass at constant temperature. For most of the tests the temperature and dew point of the gas entering and exiting the manifold were monitored.

Two sources of carrier gas were used during the spiking tests. The primary source was an oil-free ring compressor (model VFC-502P, Fuji Electric Corporation of America, Lincoln Park, New Jersey) that pumped ambient air (inlet height, 3 m) through a series of filters and into the manifold. Three large canister filters were constructed of aluminum and interconnected with 5-cm stainless steel pipe fittings. These canisters contained chemically impregnated carbon (type CA carbon and type ST carbon, Barneby and Sutcliffe Corporation, Columbus, Ohio) that was used to reduce the ammonia levels in the air stream to as low levels as possible. The filtering efficiency was about 80% initially (based on NO_y data) but degraded to the point that the lowest attainable ammonia background level was about 1 ppbv. The filters did appear to remove short-term variations in ambient levels of ammonia, which provided a more stable ammonia background than if no filters were present. Downstream of the chemical filters was a high-efficiency particulate air filter (HEPA,

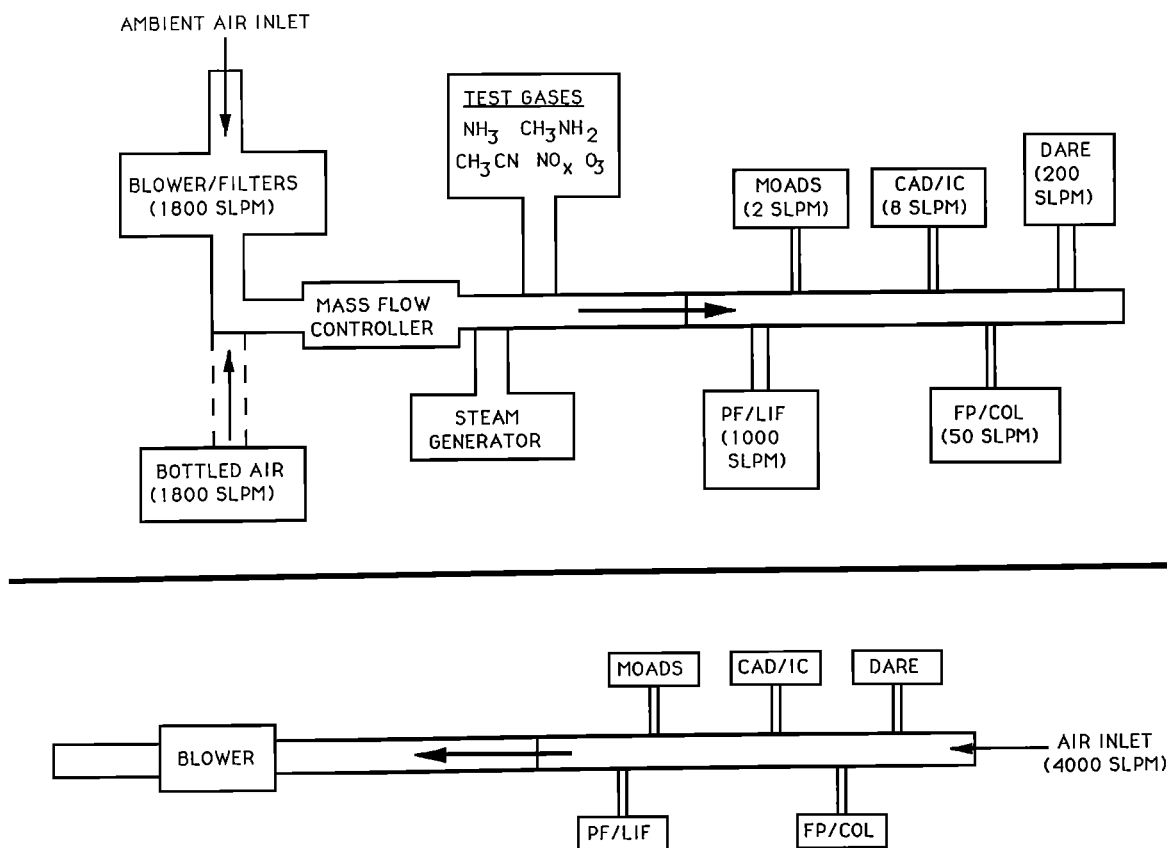


Fig. 1. Schematic diagram of the sampling manifold system. Arrows indicate the direction of the airflow. The upper panel shows the configuration for the spiking test portion of the experiment. Dashed lines from the bottled air source signify that this source was used only intermittently. The boxes show the positions along the manifold of the sampling inlets. The numbers in parentheses below the acronym for each method show the nominal flow rate for that system. The bottom panel shows the configuration of the sampling manifold during the common inlet ambient air sampling tests. The mass flow controller for total manifold flow was not used during this time.

Variflow VFA, Airguard Industries, Incorporated, Louisville, Kentucky). The second source of carrier gas was bottled zero air (General Air Service and Supply, Denver, Colorado). This air was derived from the boil-off of liquid nitrogen and liquid oxygen and blended to approximate the ratio of oxygen:nitrogen in ambient air. Because of the high flow requirements this gas was supplied from 96 cylinders of 7.3 m³ capacity each that were interconnected with a pressure-regulated manifold system. At the typical sampling manifold flow rate of 1800 L/min this gas supply lasted about 6 hours. Significant carrier gas cooling that was due to the large pressure drop and high flow rate interfered with the proper operation of the flow controller. This cooling was compensated for by routing the copper gas line through two 200-L drums that were filled with water. Downstream of the water drums the copper line was heated to bring the gas to the desired temperature. Because of the clean nature of this bottled gas no filters were placed in the gas stream.

The gas flow rate in the sampling manifold was maintained by a high-capacity flow controller (model 7500, Kurz Instruments, Incorporated, Monterey, California), which was calibrated at the factory prior to shipment. On March 8 a calibration check was performed which involved sampling the filtered ambient air stream in the glass manifold with a NO chemiluminescence detector, while the gas stream was spiked with a known quantity of NO. The spike level was calculated to be $2.66 \pm 0.11(1\sigma)$ ppbv and was detected at $2.53 \pm 0.22(1\sigma)$ ppbv. This agreement between calculated and measured NO levels indicated that the flow controller

performance was satisfactory. This test also showed that there was adequate mixing in the manifold, at least for "well-behaved" species such as NO, despite the high flow rate and short residence time (approximately 1 s). Efficient mixing is expected because the flow was in the fully turbulent realm as indicated by a Reynold's number of 22,000.

Attempts to use the NO_y instrument (gold converter/NO chemiluminescence) to obtain an independent measure of ammonia were unsuccessful, due to the very low conversion of ammonia to nitric oxide on the gold surface. However, early results of the spiking tests indicated that ammonia was well mixed with the carrier gas stream and that memory effects associated with sorption of ammonia on the walls of the glass pipe were minimal for tests with the filtered air. For the spike test at low ammonia levels (< 200 pptv, March 16), adsorption-related memory effects were more severe and required manifold cleaning prior to the spiking tests.

All of the spike compounds (except ozone and water vapor) were supplied from mixtures of the gas in air or nitrogen (Scott Specialty Gases, Longmont, Colorado). The high flow rate of carrier gas in the manifold and consequent high dilution ratios required that tank concentrations be in the range 50 to >1000 ppmv. A large dynamic range of ammonia mixing ratios was provided by a two-stage dilution system in which the ammonia tank output was first diluted in zero air; then a portion of this gas mixture was introduced into the manifold flow to achieve the desired spike level. With this system and a tank mixing ratio of 1040 ppmv, ammonia mixing ratios from 90 pptv to 57 ppbv were possible at the nominal carrier gas

flow of 1800 L/min. Propagation of error calculations using quoted tank mixing ratio uncertainties ($\pm 2\%$) and flow controller uncertainties ($\pm 2\text{--}4\%$) indicated that the error in the calculated dilution factor for the ammonia spikes was between 5% and 8%, depending on the settings of the mass flow controllers. These must be considered lower limits because of nonzero and changing background ammonia levels in the carrier gas stream.

For each of the other spike gases, except ozone and water vapor, the flow from the tank was regulated by a mass flow controller and placed directly into the manifold carrier gas stream. The uncertainties in these spike levels were about $\pm 4\%$. The methylamine and acetonitrile standards were evaluated for ammonia content by bubbling a flow of each gas through dilute acid solutions. Analyses of these solutions by ion chromatography indicated that there was substantially less than 0.5% ammonia with respect to the standard gas. Ozone at about the 4% level was generated by corona discharge through oxygen gas and introduced without further dilution into the main carrier gas stream. The final mixing ratio was monitored with a Dasibi ozone monitor and was manually adjusted to remain in the range 120–135 ppbv. Water vapor was input to the main gas flow by means of a 2.5-kW steam generator (model JR, Reimers, Clearbrook, Virginia) which was coupled to the glass manifold by a heated 6-mm OD stainless steel tube. The water input line was immediately downstream of the main mass flow controller and upstream (~ 1 m) of the inlets for the spike gases. The water for the steam generator was from a commercial deionizer and had trace levels of ammonium. This system was able to produce dew points up to about 19°C. The relative humidity of the carrier gas, then, could be varied between <10% and 73%.

2.4. Intercomparison Stages

2.4.1. Ammonia standards intercomparison. Prior to the start of the intercomparison, an evaluation of the ammonia standards used by the participants was conducted. Because gas phase (permeation devices or gas tanks) and solid phase (ammonium salts) standards were used, each group could not evaluate all of the other standards. Instead, the gas phase standards were bubbled through dilute acid solutions which were then analyzed by colorimetry and ion chromatography. Also, standard solutions used by the FP/COL and CAD/IC methods were each analyzed by the other method. In this way each standard was evaluated by one or two independent techniques, and each standard could then be checked for self-consistency with all of the others. The results from the standards intercomparison are shown in Table 1, and in all cases the agreement is better than 10%. The ammonia measurements presented below have not been normalized with respect to the standards. Finally, the ammonia standard used for the spike tests (the referee standard) was reanalyzed by ion chromatography at the end of the intercomparison. The ratio of measured ammonia to that calculated from the ammonia tank value was $0.93 \pm 0.06(1\sigma)$ for five determinations. This small loss of ammonia may be due to a change in the tank mixing ratio (i.e., wall losses) or losses in the regulator.

2.4.2. Spike gas tests. For the spiking tests the airflow was from the blower (or air cylinders) to the instrument inlet tees (see Figure 1). The spike gas lines were always under flow, either into the sample manifold or into a dump line. These gas lines were inserted directly into the carrier gas stream, and this produced equilibration times of typically 6–10 min (based on data from the PF/LIF instrument). Spike gases could be input simultaneously to the carrier gas stream in any combination, with or without the presence of water vapor. The spike tests normally were conducted over a 1.5- to 2-hour period with a half-hour equilibration time prior to the official start of the spike. These tests were conducted in a "blind" fashion in that no indication of the composition of the spike

TABLE 1. Results of the Ammonia Standards Intercomparison

| Standard Source | Evaluation Method | |
|-----------------|-----------------------|-----------------------|
| | Colorimetry | Ion Chromatography |
| Referee | 0.985 (± 0.089) | 1.005 (± 0.060) |
| MOADS | 1.034 (± 0.103) | 0.987 (± 0.079) |
| FP/COL | ... | 1.015 (± 0.061) |
| CAD/IC | 0.920 (± 0.083) | ... |
| PF/LIF | 1.082 (± 0.130) | 1.082 (± 0.087) |
| DARE | 1.029 (± 0.113) | 0.991 (± 0.069) |

Entries are the ratios of the ammonia determined by the evaluation technique to that specified by the source. Uncertainties are rms of uncertainties in the components of the ratios. PF/LIF, photofragmentation/laser-induced fluorescence. CAD/IC, citric acid denuder/ion chromatography. FP/COL, filter pack/colorimetry. DARE, denuder atmospheric research experiment. MOADS, molybdenum oxide annular denuder system.

was given to the investigators at any time. The sampled gas stream was independently monitored for temperature, dew point, ozone, and NO_y .

2.4.3. Ambient air sampling from the manifold. In addition to the spikes, ambient air was sampled from the manifold to provide homogeneous samples to the instruments (see Figure 1). During the period March 13 to March 18, except for March 16 (see spike test data), unfiltered ambient air was drawn through the manifold in the reverse sense to that of the spike tests (referred to as common inlet sampling). The manifold flow rate was not monitored during this time but was much higher than the spike tests because of the additive effect of all the instrument flows. This provided quite short residence times of gas in the manifold (<0.5 s). Sampling during these periods was closely coordinated to provide maximum overlap in the resulting data set.

2.4.4. Ambient air sampling from individual inlets. The final stage of the intercomparison was a sampling period from March 20 to March 29 during which each instrument was configured as closely as possible to normal field operation. The inlets were placed 5 m above ground and as close together as possible. Sampling was continuous in order to have as large a data base as possible. Because the sampling times of the CAD/IC and FP/COL methods were substantially longer than the other methods, sampling periods were identical between these two techniques. Any anticipated downtime of the other instruments was scheduled to occur between the sampling periods of the CAD/IC and FP/COL methods for maximum data overlap. Finally, as with the common inlet sampling period, many other chemical and meteorological parameters were measured simultaneously with ammonia.

3. Results of the Spiking Tests

Table 2 is a summary of all of the spike test results. The table lists calculated means and standard deviations (1σ) of reported NH_3 mixing ratios for the PF/LIF, MOADS, and DARE methods and the NH_3 determinations from the CAD/IC and FP/COL methods for each of the test periods. The numbers in parentheses for CAD/IC and FP/COL are the uncertainties given by the investigators. The spike gas levels were calculated from the tank concentrations and dilution ratios derived from the mass flow controller settings. The following discussion will outline the data reduction techniques and then describe the results from each instrument. The data in Table 2 will be discussed in three respects: ammonia spike results

TABLE 2. Mean Measured Ammonia

| Date | Start Time | Stop Time | Carrier Gas | Carrier Gas Temp./RH | Spike Gas, pptv |
|----------|------------|-----------|-------------|----------------------|--|
| Feb. 28 | 1030 | 1230 | F | 23.7/11 | |
| Feb. 28 | 1300 | 1500 | F | 24.1/10 | NH ₃ , 14300 |
| Feb. 28 | 1600 | 1800 | F | 23.7/10 | NH ₃ , 5590 |
| March 1 | 1200 | 1400 | F | 28.0/35 | NH ₃ , 11400 |
| March 1 | 1500 | 1700 | F | 28.0/60 | NH ₃ , 11400 |
| March 3 | 0930 | 1100 | F | 22.7/ 7 | |
| March 3 | 1130 | 1300 | F | 24.5/ 6 | NH ₃ , 3120 |
| March 3 | 1330 | 1500 | F | 23.9/ 7 | NH ₃ , 6830 |
| March 6 | 1100 | 1230 | F | 32.6/35 | NH ₃ , 6050 |
| March 6 | 1300 | 1430 | F | 33.2/43 | NH ₃ , 6050 |
| March 7 | 1030 | 1200 | B | 20.0/73 | NH ₃ , 3590; CH ₃ NH ₂ , 3020 |
| March 7 | 1230 | 1400 | B | 20.0/73 | CH ₃ NH ₂ , 3020 |
| March 7 | 1430 | 1500 | B | 20.0/73 | |
| March 8 | 1200 | 1330 | F | 37.3/12 | |
| March 8 | 1400 | 1530 | F | 37.3/12 | NO, 2660; NO ₂ , 5350 |
| March 9 | 1200 | 1330 | F | | |
| March 9 | 1400 | 1530 | F | | O ₃ , 120-135 (ppbv) |
| March 10 | 1030 | 1200 | B | 20.0/<10 | |
| March 10 | 1230 | 1400 | B | 20.0/73 | |
| March 10 | 1430 | 1600 | B | 20.0/73 | NH ₃ , 2660 |
| March 11 | 0830 | 1000 | F | | |
| March 11 | 1030 | 1200 | F | | CH ₃ CN, 2890 |
| March 13 | 1230 | 1400 | F | 36.0/37 | |
| March 13 | 1430 | 1600 | F | 39.0/31 | CH ₃ NH ₂ , 2950 |
| March 16 | 1230 | 1330 | B | 24.0/<10 | |
| March 16 | 1330 | 1430 | B | 24.0/<10 | NH ₃ , 109 |
| March 16 | 1430 | 1530 | B | 24.0/<10 | NH ₃ , 338 |
| March 16 | 1530 | 1630 | B | 24.0/<10 | NH ₃ , 181 |
| March 16 | 1630 | 1730 | B | 24.0/<10 | |

Times are mountain standard time (MST). F, filtered air; B, bottled air; (...), in percent. Numbers in parentheses are 1 sigma standard deviations. Numbers in

(Table 3), measured background ammonia in the carrier gas, and other spike results (Table 4).

As discussed earlier, each of the spikes was a standard addition to the carrier gas stream which contained an unknown and often changing level of background ammonia. In general, the format for each of these tests was similar: a determination of the background ammonia level was followed by a measurement with added spike gas. In order to use the concentration of the spiked compound as a reference, the background level must be subtracted from the total spike level determined by each instrument. This background level can only be estimated from the measurements by the five intercompared techniques. These results were not always in agreement. Hence two aspects of the spiking tests must be discussed for each technique: the background measured and the increase above this measured background due to the response of the instrument to the added spike gas.

For many of the filtered air tests the background levels were reasonably constant, so both background and spiked levels are adequately represented by the arithmetic means for the test periods. The mean background level could then be subtracted from the mean spiked level to get the measured response to a spike, and this response is reported in Tables 3 and 4. The uncertainty for the response was calculated as the

root mean square of the sum of the standard errors of the means, where the standard errors were estimated from standard deviations and numbers of data points in the test periods. The fraction of added ammonia (or other spike gas measured as ammonia) that was determined by each technique (referred to as the fractional recovery and included in Tables 3 and 4) is the ratio of measured spike gas to that added, which was calculated from the dilution ratio. This assumes that there were no wall (or other) losses and that the background levels remained constant.

Changing backgrounds were evident in all of the bottled air spike data, so additional methods of data reduction were employed. An example of this is shown in Figures 2 and 3, which depict the data for March 16. The test protocol involved the use of dry zero air with no added gases other than ammonia. Because of the low ammonia levels used during this test the CAD/IC and FP/COL methods collected one sample over the entire 5-hour period; thus the stepwise changes in added ammonia levels shown in Table 2 are not listed for those two methods. Figure 2 shows the data from the PF/LIF, CAD/IC, and FP/COL instruments as well as the mixing ratios of added ammonia. The lower part of the figure shows the changing background as determined by the PF/LIF instrument. This temporal trend suggests the use of interpolated

Mixing Ratios for Spike Tests, pptv

| PF/LIF | CAD/IC | FP/COL | DARE | MOADS |
|-------------|-------------|------------|-------------|-------------|
| 384(71) | 440[130] | 70[280] | No data | 183(19) |
| 12332(982) | 11760[1180] | 2900[1160] | No data | 4620(894) |
| 5532(475) | 4980[510] | 1900[760] | No data | 2095(291) |
| 10338(1010) | 2200[240] | 4300[1720] | 6574(363) | 5378(715) |
| 9235(1291) | 310[130] | 4900[1960] | 5168(893) | 13833(4895) |
| 1022(100) | 190[120] | 670[442] | 90(0) | 297(33) |
| 3780(301) | 3530[370] | 1500[585] | 1442(482) | 1560(128) |
| 6690(476) | 7320[1000] | 1300[507] | 6403(324) | 3120(428) |
| NO DATA | 9500[950] | 5100[2040] | 1394(202) | No data |
| NO DATA | 3870[390] | 4030[1572] | 1312(353) | No data |
| 5822(691) | 5970[610] | 2700[1053] | 11878(1447) | 11890(1486) |
| 2349(388) | 1210[160] | 1200[480] | 15803(814) | 5570(572) |
| 1752(663) | 3420[450] | 1300[507] | 13723(544) | 4880(0) |
| 2244(473) | 2020[230] | 720[288] | 1802(694) | 1733(494) |
| 1471(359) | 880[180] | 1200[708] | <100 | 820(62) |
| 962(103) | 1380[170] | 404[182] | 992(661) | 1000(57) |
| 967(110) | 1120[150] | 510[230] | <100 | 820(62) |
| 105(17) | 90[100] | 120[92] | 367(181) | 320(62) |
| 1623(615) | 2020[250] | 1500[1470] | 5880(393) | 2547(800) |
| 3163(266) | 3790[400] | 1700[765] | 6534(347) | 7280(459) |
| 1083(217) | 1380[150] | 760[304] | <100 | 1353(988) |
| 1655(202) | 1430[150] | 490[191] | <100 | 1517(184) |
| 1061(184) | 410[170] | 605[430] | <100 | 1287(90) |
| 1063(207) | 1050[150] | 690[352] | <100 | 1843(116) |
| 202(21) | ... | ... | 630(70) | 1670(400) |
| 255(22) | ... | ... | 603(55) | 985(125) |
| 496(51) | 180[30] | 88[35] | 647(12) | 930(90) |
| 321(24) | ... | ... | 613(48) | 675(50) |
| 93(26) | ... | ... | 473(56) | 445(35) |

could not be determined. Temperature in degrees Celsius; RH, relative humidity, is brackets refer to uncertainties as defined in the experimental section for the method.

background levels, rather than an average background, for data evaluation here. A trend line for the background was established by linear least squares fit through the PF/LIF data at the end of the first period (1315–1330 MST) and data at the end of the final period (1700–1730 MST). Background levels at the midpoints of the intermediate test periods (i.e., at 1400, 1500, and 1600 MST) were determined from the trend line and subtracted from the mean spiked ammonia levels at the same point in time. The uncertainties were calculated as described above. For the CAD/IC and FP/COL methods, two fractional recoveries for the spike are given. These fractions differ in that one was calculated with the background estimated from the PF/LIF data (lower estimate) and the other calculated with an assumed zero background (upper estimate). Figure 3 shows the March 16 data for the MOADS and DARE methods. For these two cases no reliable determination of the fractional recovery was possible.

Similar data analysis was applied to the two other bottled air tests. There was some ambiguity in the calculation of the background level to subtract from the level measured during the spike, and therefore upper and lower estimates were calculated and reported in Table 3.

3.1. PF/LIF Ammonia Spike Results

The data set from the PF/LIF instrument is the most consistent with the calculated added ammonia spikes (see Table 3). The average of the measured ammonia in the filtered air tests was 87% of that added with a relative standard deviation (RSD, 1σ) of 5%. The bottled air results are consistent with this same recovery, although there is an indication of a higher mean value (the average of all fractional recovery determinations in bottled air including upper and lower bounds is 98% with an RSD of 19%). Overall, these results indicate that the PF/LIF instrument can determine ammonia with a high degree of accuracy over a wide range of mixing ratios (100 pptv to >14 ppbv). An approximate measure of instrument precision can be estimated from the overall relative standard deviation (17%). This value is an upper limit since much of the uncertainty in background determinations was due to the manifold system and not the instrument.

3.2. CAD/IC Ammonia Spike Results

The CAD/IC data in Table 3 indicate a 93% fractional recovery with a relative standard deviation of 16% in the

TABLE 3. Recovered Mean (Standard Error) Ammonia, pptv, and Fractional Recovery of Added Spike Gas

| Date | Start Time | Stop Time | Carrier Gas Temp./RH | Spike Gas, pptv | PF/LIF | CAD/IC | FP/COL | DARE | MOADS |
|---------------------|------------|-----------|----------------------|-------------------------|--------------------|---------------------|--------------------|-------------------|-------------------|
| <u>Filtered Air</u> | | | | | | | | | |
| Feb. 28 | 1300 | 1500 | 24.1/10 | NH ₃ , 14300 | 11948(159) 0.84 | 11320(1187) 0.79 | 2830(1193) 0.20 | No data | 4437(46) 0.31 |
| Feb. 28 | 1600 | 1800 | 23.7/10 | NH ₃ , 5590 | 5148(51) 0.92 | 4540(526) 0.81 | 1830(810) 0.33 | No data | 1912(145) 0.34 |
| March 3 | 1130 | 1300 | 24.5/6 | NH ₃ , 3120 | 2758(40) 0.88 | 3340(389) 1.07 | 830(733) 0.27 | 1352(216) 0.43 | 1263(76) 0.41 |
| March 3 | 1330 | 1500 | 23.9/7 | NH ₃ , 6830 | 5668(64) 0.83 | 7130(1007) 1.04 | 630(673) 0.092 | 6313(122) 0.92 | 2823(248) 0.41 |
| <u>Bottled Air</u> | | | | | | | | | |
| March 7 | 1030 | 1200 | 20.0/73 | NH ₃ , 3590" | 3473* 0.97 | 4760* 1.33 | 1500* 0.42 | -2340* -0.65 | 8760* 2.44 |
| March 10 | 1430 | 1600 | 20.0/73 | NH ₃ , 2660 | 2350† 0.66 | 2498† 0.70 | 0† 0 | -3925† -1.09 | 6320† 1.76 |
| | | | | | 3030* 1.14 | 3349* 1.26 | 1259* 0.47 | 654 0.25 | 7147* 2.69 |
| | | | | | 2394† 0.90 | 1770† 0.67 | 200† 0.075 | | 4733† 1.78 |
| March 16 | 1330 | 1430 | 24.0/<10 | NH ₃ , 109 | 97 0.89 | † † | † † | † † | † † |
| March 16 | 1430 | 1530 | 24.0/<10 | NH ₃ , 338 | 365 1.07 | † † | † † | † † | † † |
| March 16 | 1530 | 1630 | 24.0/<10 | NH ₃ , 181 | 220 | 180 | 88 | † | † |
| | | | | | 1.22 | 0.687-1.429§ | 0.305-0.635§ | | |

Times are mountain standard time (MST). Temperature, in degree Celsius; RH, in percent.

*Upper limit.

†Lower limit.

‡Could not be determined.

§Calculated with background level as determined by PF/LIF or with assumed zero background.

3020 pptv CH₃NH₂ also present during spike and background determinations.

TABLE 4. Recovered Mean (Standard Error) Spike Gases as Ammonia, pptv, and Fractional Recovery of Added Spike Gas

| Date | Start Time | Stop Time | Carrier Gas Temp./RH | Spike Gas, pptv | PE/LIF | CAD/IC | FP/COL | DARE | MOADS |
|--|------------|-----------|----------------------|--|-------------------|---------------------|-------------------|-------------------|--------------------|
| <u>Filtered Air Tests</u> | | | | | | | | | |
| March 8 | 1400 | 1530 | 37.3/12 | NO, 2660/NO ₂ , 5350 | ... | ... | ... | ... | ... |
| March 9 | 1400 | 1530 | | O ₃ , 120-135 (ppbv) | 5(23) 0.000 | -260(227) -0.002 | 106(293) 0.001 | -892(-) -0.007 | -173(47) -0.001 |
| March 11 | 1030 | 1200 | | CH ₃ CN, 2890 | ... | ... | ... | ... | ... |
| March 13 | 1430 | 1600 | 39.0/31 | CH ₃ NH ₂ , 2950 | 2(34) 0.000 | -360(227) -0.12 | 85(556) 0.029 | ... | 566(85) 0.19 |
| <u>Bottled Air Tests</u> | | | | | | | | | |
| March 7 | 1230 | 1400 | 20.0/73 | CH ₃ NH ₂ , 3020 | 250(192) 0.083 | ... | ... | ... | ... |
| <u>Relative Humidity Effects (Mean and s.d., pptv)</u> | | | | | | | | | |
| March 1 | 1200 | 1400 | 28.0/35 | NH ₃ , 11400 | 10338(1010) | 2200(240) | 4300(1720) | 6574(363) | 5378(715) |
| March 1 | 1500 | 1700 | 28.0/60 | NH ₃ , 11400 | 9235(1291) | 310(130) | 4900(1960) | 5168(893) | 13833(4895) |
| March 6 | 1100 | 1230 | 32.6/35 | NH ₃ , 6050 | No data | 9500(950) | 5100(2040) | 1394(202) | No data |
| March 6 | 1300 | 1430 | 33.2/43 | NH ₃ , 6050 | No data | 3870(390) | 4030(1572) | 1312(390) | No data |

Times are mountain standard time (MST). Temperature in degrees Celsius; RH in percent. (...), could not be determined.

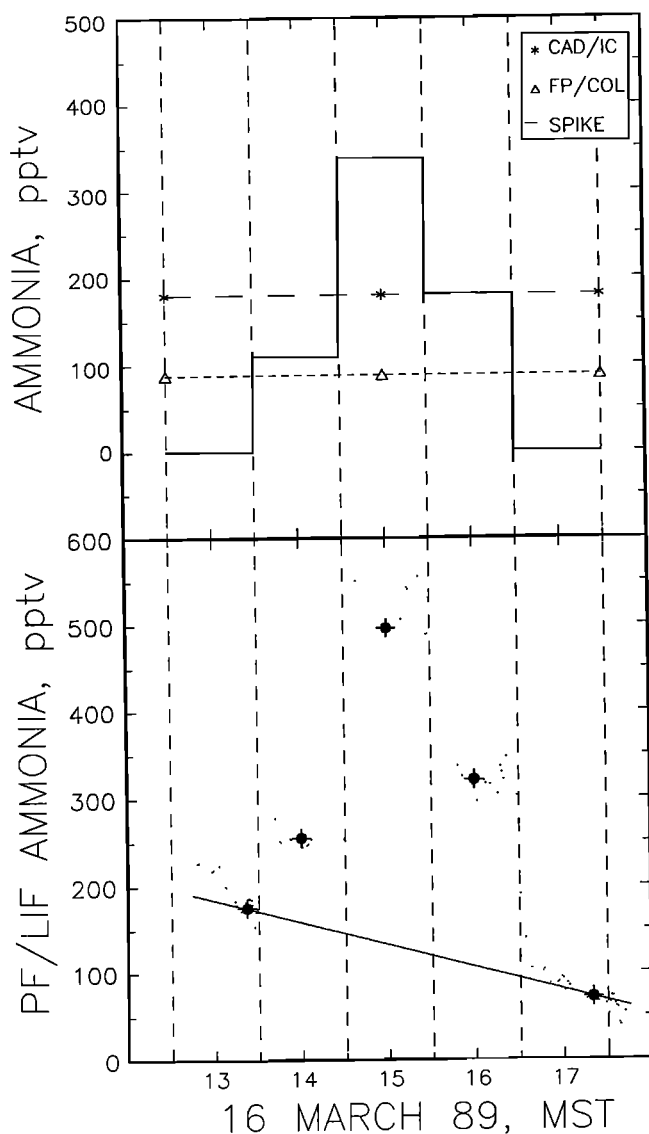


Fig. 2. Data from the bottled air spike test of March 16. The vertical dashed lines signify the start and stop times of the tests as well as the times when the added ammonia spikes were changed. The upper panel depicts the levels of added ammonia (solid line) and the 5-hour integrated data from the citric acid denuder/ion chromatography (CAD/IC) and filter pack/colorimetry (FP/COL) techniques. The lower panel shows the data from the photofragmentation/laser-induced fluorescence (PF/LIF) system. The heavy symbols within the data clusters are the means of each cluster. The solid line is the linear least squares fit between the background data at the start of the test and that at the end of the test.

filtered air tests. Thus this technique also accurately measures ammonia, at least at the relatively high levels of the filtered air tests. It should be noted that the filtered air recoveries are similar during each individual day but quite different between the two days. These trends may indicate the influence of the blank determination on individual measurements.

The results from the three bottled air tests give lower and upper estimates that include unity for the ammonia recovery. Thus there is no indication of any inaccuracy in the measurement of average ammonia levels down to about 200 pptv. The changing background levels in the bottled air tests are responsible for the relatively wide limits on the calculated recoveries. For example, the data in Table 2 for the test on March 10 show comparable average levels for the CAD/IC and

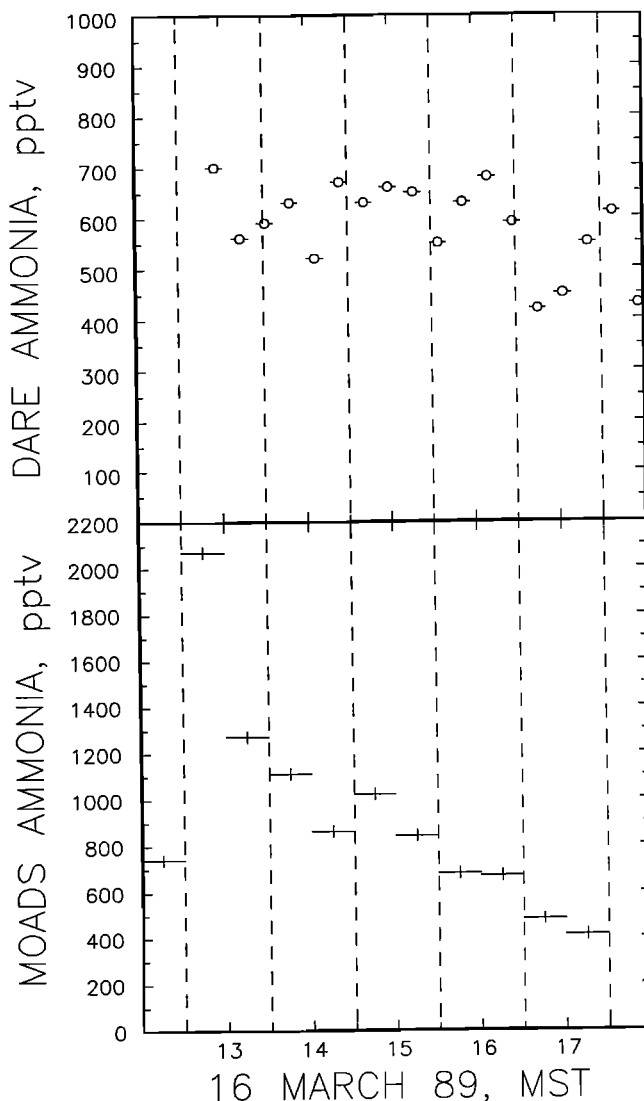


Fig. 3. Data from the bottled air spike test of March 16 from the denuder atmospheric research experiment (DARE) (upper panel) and molybdenum oxide annular denuder system (MOADS) (lower panel) instruments. The horizontal lines through the data points show the time over which each sample was integrated (10 min for DARE and 30 min for MOADS). Note that the y axis scale is different between the upper and lower panels and also different from those in Figure 3.

PF/LIF techniques for each test period. The change in the average level when the ammonia was added agreed to within 15% between the two techniques. However, the raw PF/LIF (and MOADS) data show the ammonia levels coming to stable values only at the end of the test period after the humidity had been increased. Because the CAD/IC technique must sample over the entire test period, the ammonia measured by it will not be representative of the stable value found at the end of the test period. The same considerations apply to the FP/COL technique discussed in the next paragraph. The consequence is that accurate fractional recoveries cannot be calculated unless the ammonia levels are constant during both the spike and the background periods.

3.3. FP/COL Ammonia Spike Results

For the FP/COL method the mean recovery in the filtered air tests was 22% with a relative standard deviation of 46%. The upper and lower estimates from the bottled air tests

indicate low average recoveries as well. It may be the case that under the conditions of these tests the collection efficiency of this method is low. This is not an unexpected result since previous laboratory tests have shown that the collection efficiency becomes less than unity at relative humidity levels lower than about 75% [Quinn and Bates, 1989]. However, the data in Table 2 suggest that a factor or factors other than relative humidity may influence the ammonia levels that are determined by this method. On March 10 there is reasonably good agreement of the FP/COL data with the CAD/IC data and the average PF/LIF data during the first two test periods when the relative humidity was changed from less than 10% to 73%. At the high humidity level when unit collection efficiency would be expected for the FP/COL technique, the observed ammonia recovery was less than 50%. These low recoveries will be discussed in more detail in section 4. In summary, the ammonia spike tests indicate that ambient measurements by this technique under these conditions may be systematically low.

3.4. MOADS Ammonia Spike Results

The MOADS filtered air results in Table 3 show an average recovery of 37% of the added ammonia with a relative standard deviation of 14%. The two bottled air tests with interpretable results gave upper and lower bounds that indicate a recovery greater than unity (approximately 200%). In some cases the two denuder channels in this system gave different results. In contrast to the large differences seen in the mean spike levels, the MOADS and the PF/LIF data exhibit qualitative agreement, in most cases, with respect to temporal variations of background and spiked ammonia levels. Also, prior to March 6 the MOADS data are systematically lower than the PF/LIF data, but after March 6 the measured levels agree with or are greater than the PF/LIF data. While these results suggest a possible calibration problem with the MOADS system, whether or not there is agreement also appears to depend on the nature of the carrier gas (bottled or filtered) and the relative humidity. This strongly suggests that collection and/or conversion of ammonia in this denuder system is sensitive to changes in the characteristics of the air that is sampled. Such effects might be anticipated in some ambient conditions.

3.5. DARE Ammonia Spike Results

For this method the average of the two filtered air data points in Table 3 is 68% with a 51% RSD. The raw data suggest that the DARE system and/or manifold was not equilibrated during the first of these two tests. The result from one bottled air test is 25% and apparently negative in the other. In general the DARE and PF/LIF data do not track temporal variations in ammonia spikes and background ammonia levels. One possible explanation for these inconclusive results is that the inlet line used to draw samples from the main manifold flow influenced the composition of the sample. As will be seen in the following sections, similar behavior was observed in the common inlet ambient data (which also was acquired from sampling through the manifold) but not seen in the separate inlet ambient air data. These observations will be considered further in the summary section at the end of the paper.

3.6. Determinations of Background Ammonia in Carrier Gas

The above results can be used to examine the background ammonia levels in the carrier gas. The PF/LIF and the CAD/IC techniques, which both showed about 90% recovery of the ammonia spikes, gave similar results for the background determinations; for the nine common measurements in Table 2 the average CAD/IC to PF/LIF ratio was 1.15 with a relative standard deviation of 42%. The FP/COL technique generally gave lower results for the background levels; the average

FP/COL to PF/LIF ratio was 0.63 with a relative standard deviation of 47%. This low ratio is in approximate accord with the lower fractional ammonia recovery found above for the FP/COL system and is in excellent agreement with the FP/COL to PF/LIF ratio from the ambient measurements discussed below. The MOADS and PF/LIF data show qualitative agreement with respect to the trends and variations in the background levels. These results are all self-consistent and indicate a reasonably well defined background of ammonia in the carrier gas. This being the case, several conclusions can be drawn concerning the reasons for variation of background levels. (1) The large variations observed for the filtered air background ammonia are undoubtedly due to poor filter efficiency since this variability was almost completely removed with bottled air. The trends seen in the bottled air background ammonia levels are consistent with desorption of ammonia from the walls of the glass manifold. (2) Related to this last point is the large-scale desorption of ammonia due to displacement by water when the carrier gas relative humidity was increased. This effect, which has been observed elsewhere [Adema et al., 1990], is most noticeable in the data from March 10. (3) There is an indication that ammonia may be scavenged or sequestered by water vapor at high relative humidities. This is suggested by the data from the March 1, 7, and 10 spike tests and is supported by data from one period during ambient sampling (see below). These effects have implications for the common inlet stage of the intercomparison, which is discussed below.

3.7. Interferant Spike Tests

Table 4 gives the results of the spike tests with compounds that are potential interferants in the ammonia determinations. They can be succinctly summarized as giving no persuasive evidence for any interferences in any of the systems. However, changing background levels generally prevented stringent upper limits from being placed on the possible extent of the interferences.

Methylamine was thought to be a particularly important gas to test since it is chemically similar to ammonia and is also found in the troposphere. Spike tests of this compound were conducted with humidified filtered air and humidified bottled air. The filtered air test indicated no interferences except for a possible 19% positive interference from methylamine in the MOADS instrument, but more data are needed to substantiate this. During the one bottled air test changing background levels and carrier gas flow instability (due to low gas tank pressure) were such that the data cannot be interpreted.

During the O₃ test the ammonia background in the filtered air, as indicated by the PF/LIF results, remained very constant. No interference from ozone was seen in any of the instruments. Because of the constant background, relatively stringent limits can be placed on the magnitude of possible interferences. In contrast, during the NO_x and CH₃CN tests the PF/LIF data indicate that the ammonia levels in the filtered air changed dramatically, which resulted in negative (for NO_x) and positive (for CH₃CN) apparent interferences as calculated from the averages of the reported ammonia levels. No conclusions can be made based on these results.

For the relative humidity tests a constant level of ammonia was added to the carrier gas while the dew point was varied. No separate determinations of the ammonia background with and without added water vapor were made during these tests. The results are listed in Table 4 as the mean ammonia mixing ratios over the spike test period. A concern during these tests was that the background ammonia level would increase due to the presence of ammonia (or ammonium salts) in the steam generator feed water supply. Every attempt was made to minimize this effect by keeping the steam generator and the supply water clean and by using a relatively high spiking level of ammonia. However, data from the test on March 10 suggested that this effect was small and was overwhelmed by

the displacement by water vapor of ammonia from the manifold walls.

For these relative humidity tests no fractional recoveries for ammonia could be calculated because data on the ammonia background levels were not available. During the humidity tests the mean ammonia mixing ratios as determined by all of the instruments (with two exceptions, see Table 4), were lower than the calculated ammonia spikes, even if the background levels are assumed to be zero. Part of the cause of these low levels may well be due to ammonia losses in the manifold before sampling. Also, the data collected at high humidity exhibit more scatter. Thus the apparent interference by water vapor may be due to several factors: changes in background ammonia, more severe losses in the sampling manifold at high humidity, and differences in the responses of the instruments.

Given the uncertainties in the tests, no significant change in the performance of the PF/LIF instrument with relative humidity was found. The CAD/IC results from March 1 must be discounted because of water condensation on the inlet of the denuder tube. The ambient temperature on this day was below freezing, and the heating and insulation of the sampling manifold at the CAD/IC inlet were not sufficient to prevent condensation from occurring when the carrier gas relative humidity was high. This problem was corrected by March 6, and the inconsistent results (apparent ammonia recoveries of 1.57 and 0.64, assuming zero background ammonia) from this test are not understood. The FP/COL results show that measured ammonia levels do not change significantly with large changes in relative humidity, but the absolute recovery of ammonia appears to be consistently low regardless of the relative humidity. Similar behavior is seen in the DARE data for these tests. The absolute levels on March 6 are considerably less than the calculated spike levels, but these may be indicative of losses in the DARE sampling transfer line. The MOADS system exhibits an apparent increase in ammonia with higher relative humidity. However, as with the CAD/IC system on March 1, condensation on the MOADS inlets probably influenced the measurements. This is also indicated by the much higher ammonia levels determined by one of the MOADS denuders with respect to the other. This behavior was observed during one period of ambient sampling under conditions similar to those of this test and will be discussed in detail below.

4. Discussion of Ambient Air Measurements

Three episodes from the ambient air measurement period illustrate the performance of the ammonia instruments under widely different atmospheric conditions. The first episode, which is typical of the instrument agreement, began at 0600 MST on March 27 and ended at 1200 MST on March 28. Figure 4 shows the measured ammonia levels and the meteorological conditions, which were characterized by moderate temperature, low relative humidity (except for one period), and variable winds. The measured ammonia levels varied from about 300 pptv to about 8 ppbv with the lowest levels associated with westerly winds. In general, agreement to better than a factor of 2 was seen among all the ammonia instruments at all times, even when large changes in the ammonia mixing ratio occurred over very short time intervals. This especially is noticeable at about 2000 MST on March 27 when the strong westerly winds subsided. Concurrent changes also occurred in the relative humidity and temperature. During a brief period of north wind the ammonia mixing ratio as measured by the PF/LIF instrument increased from about 300 pptv to more than 5 ppbv in less than 10 min. Nevertheless, each of the three instruments that make continuous measurements (DARE, MOADS, and PF/LIF) observed a comparable increase in the ammonia level. Over the subsequent period of decreasing ammonia, short-term

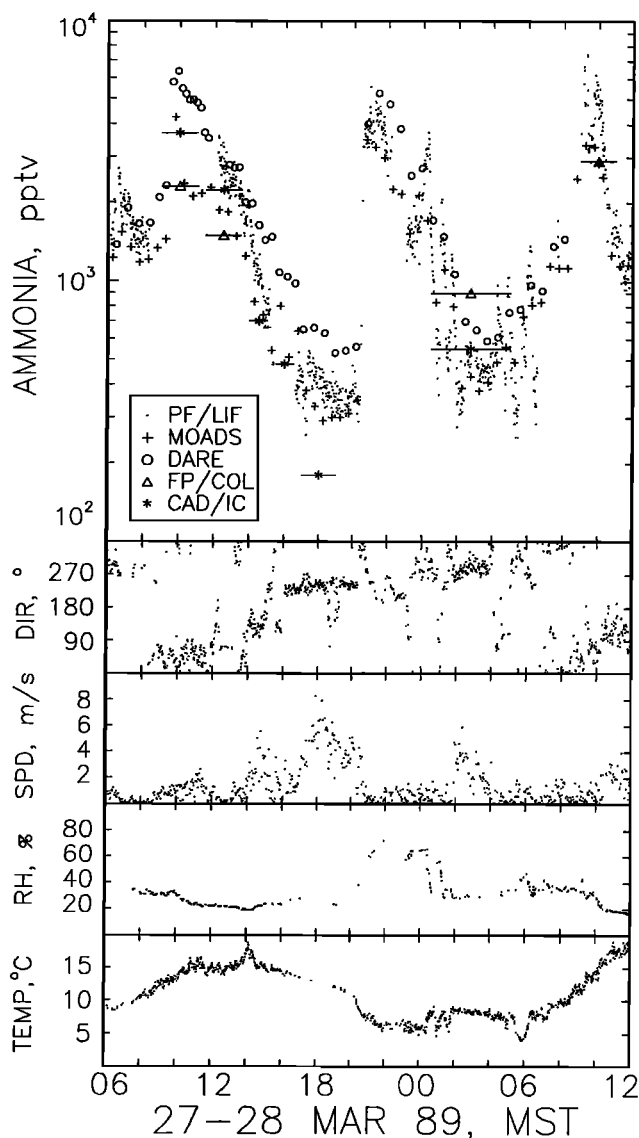


Fig. 4. Data from the ambient air sampling period of 0600 MST on March 27 to 1200 MST on March 28. The horizontal bars on the FP/COL and CAD/IC data show the sampling times for each point.

fluctuations are evident, which were also tracked by these three instruments.

Figure 5 presents the data for the period of lowest ambient ammonia (except for a period of fog, described below). During the 24-hour period beginning 0900 MST on March 14 moderate to strong downslope (westerly) winds brought air with low ammonia levels to the site. The five ammonia detectors were sampling from the common manifold at this time. The upper panel indicates that all of the systems were measuring levels that averaged below 200 pptv throughout the period. However, the mean of the FP/COL data is less than that of the DARE, CAD/IC, and PF/LIF systems, while the mean of the MOADS data is substantially greater. The mean values of the other three data sets agree to within about 30% of one another (28 pptv absolute). Two of the systems (PF/LIF and MOADS) show very similar temporal trends, relatively low until 1700, a modest spike between 1700 and 2100, and a return to low values at 2200 followed by gradually increasing levels. While short-term trends cannot be discerned in the FP/COL and CAD/IC data, there appears to be qualitative agreement over the long term between data from these methods

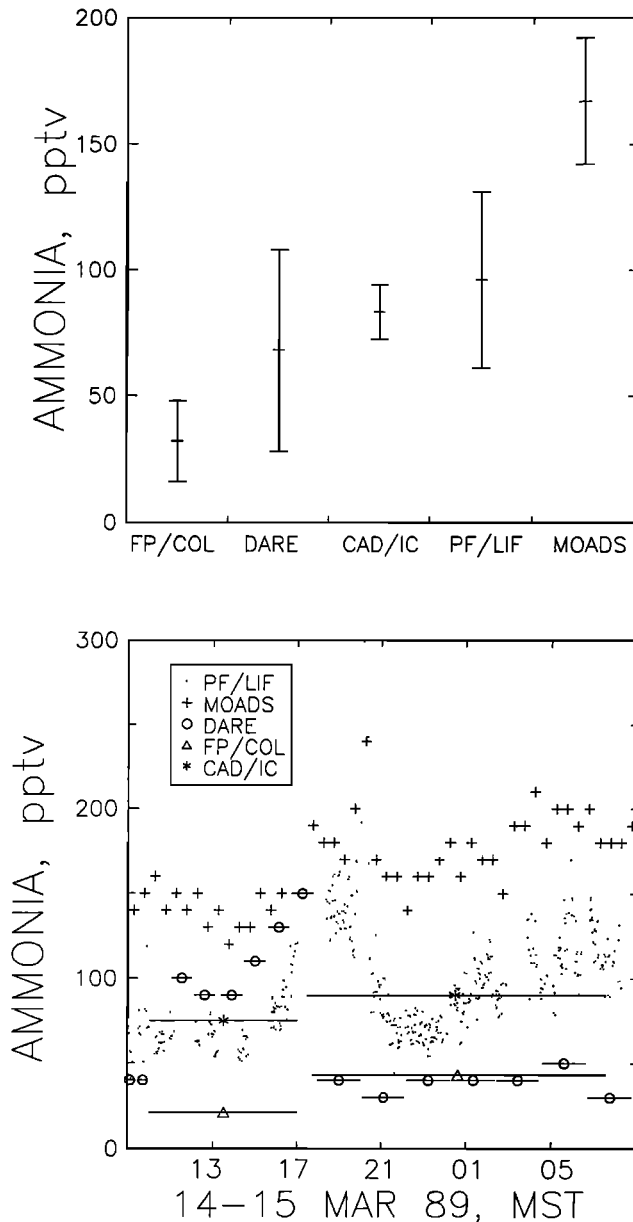


Fig. 5. The lower panel shows data from the common inlet ambient air sampling period from 0900 MST on March 14 to 0900 MST on March 15. The horizontal bars on the FP/COL and CAD/IC data indicate the sampling times for each point. The upper panel shows the average ammonia mixing ratios and the (1σ) standard deviations for each instrument over this 24-hour period.

and that from the PF/LIF system. Consistent with the averages discussed below, the MOADS and FP/COL data are offset, respectively, above and below data from the PF/LIF and CAD/IC methods. The DARE system does not show the same temporal trend as the PF/LIF data for the entire period, but there does appear to be some similarity between 1300 and 1700. The peak between 1700 and 2100 is not indicated and constant low values are observed during the last two thirds of the period. However, these data may have been influenced by the transfer line which drew sample air from the main manifold system during this period. This will be discussed further below. In general, however, all five systems are in good agreement considering the low ammonia levels measured.

A substantially different episode, shown in Figure 6, occurred from 1000 MST on March 20 to 1800 MST on March 21. This period was characterized by low temperature, high relative humidity, and generally light to calm winds. During part of this period the site was enveloped in fog, which coincided with large differences in measured ammonia levels among the instruments. Under these conditions the MOADS instrument in particular reported much higher ammonia levels than did the other systems, and there was a marked divergence in the levels determined by the two different measurement channels of this instrument. Similar behavior was seen for the MOADS system during a spike test at high relative humidity. These differences became quite small again when the temperature increased and the relative humidity decreased.

One possible reason for the high values reported by the MOADS instrument is that this instrument has a greater sensitivity to certain ammonia-containing aerosols than does the PF/LIF technique. Ammonium sulfate is not likely to

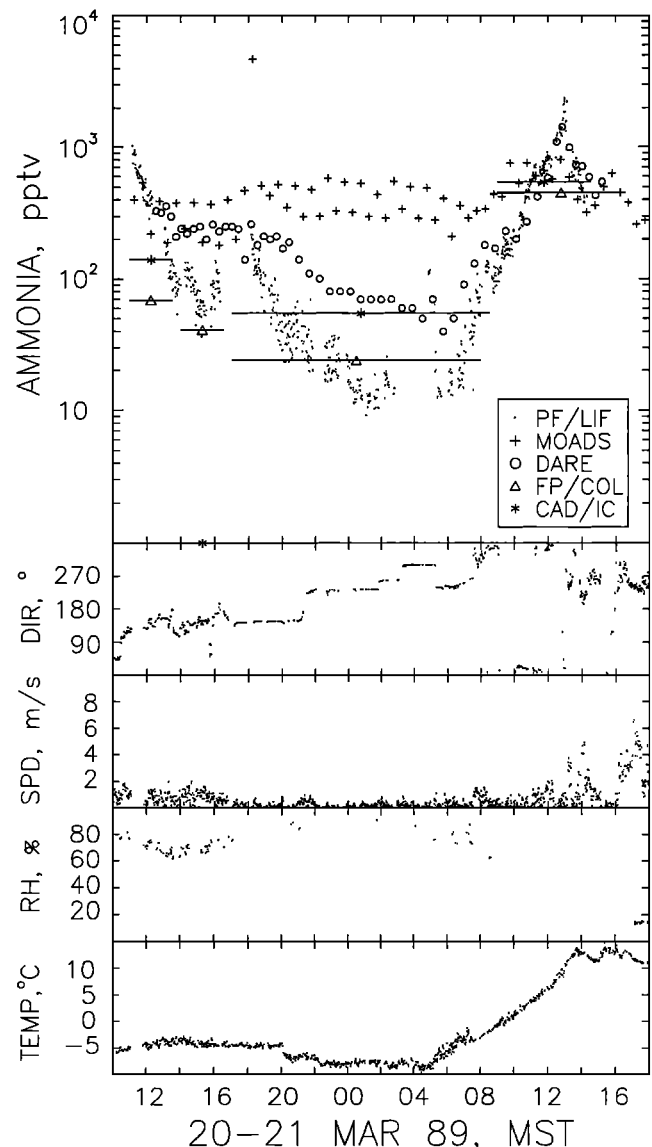


Fig. 6. Data from the ambient air sampling period from 1000 MST on March 20 to 1800 MST on March 21. The horizontal bars on the FP/COL and CAD/IC data show the sampling times for each point.

contribute to an ammonia interference in the MOADS instrument since ammonia will not be volatilized from $(\text{NH}_4)_2\text{SO}_4$ at the sampling temperature, but ammonium nitrate is sufficiently labile to release ammonia [Finlayson-Pitts and Pitts, 1986]. However, particulate ammonium and particulate nitrate were at a maximum at the beginning of the period and then decreased. Further, a plot of the difference (MOADS - PF/LIF) versus particulate ammonium for the total ambient sampling period shows no correlation, while a similar plot versus particulate nitrate shows, if any, a negative correlation. This suggests that the divergence of the MOADS results from the other data is probably not due to particulate ammonium.

An alternative explanation is that fog droplets and/or ice crystals scavenged gaseous ammonia which was subsequently released when drawn into the warmed MOADS inlets. At the temperatures observed (-5° to -8°C) the probability is less than 40% of ice crystals being detected [Wallace and Hobbs, 1977]. However, observations by one of us (J. Bradshaw) of unusual light refraction and scattering after midnight suggest that some ice crystals were present. Thus it is likely that the fog was a mixture of supercooled water droplets and ice crystals. Partitioning of ammonia into the aqueous phase can be estimated from Henry's law theory. If reasonable assumptions are made of PH (5.5, which is characteristic of Sugarloaf Mountain rain during March 1988 [National Atmospheric Deposition Program (NADP), 1989]), relative water content (approximately $10^{-6} \text{ m}^3 \text{ H}_2\text{O m}^{-3} \text{ air}$ for clouds or fog), and an effective Henry's law constant of $5 \times 10^5 \text{ M atm}^{-1}$, then $\geq 90\%$ of gaseous ammonia will be partitioned into the aqueous phase. This calculation is similar to that of Seinfeld [1986]. When these ammonia-laden droplets were drawn into the heated inlet (50°C) of the MOADS instrument, the dissolved ammonia was partially released (due to the higher vapor pressure of ammonia at the higher temperature) and collected by the denuder tubes. The differences seen in measured ammonia between the two MOADS denuder tubes may be related to differences in inlet and/or denuder temperatures. Evidence for the scavenging of gas phase NH_3 can be seen from the strong correlation between the increase in relative humidity and the decrease in ammonia that was determined by the PF/LIF system. Revolatilization of ammonia from droplets would be expected for any inlet or sampling system that was heated to greater than ambient temperature.

To compare the results from the different systems, each of the instruments individually will be compared to the PF/LIF system. The PF/LIF data were chosen as the primary basis for comparison because this instrument showed the best overall agreement with the ammonia standard additions in the spiking tests (with no interferences) and the PF/LIF method has the finest time resolution (1 min). All of the other techniques required longer sampling times, and with one exception, exact overlap of the sampling periods of the various techniques did not occur. Thus in order to make comparisons with other than the PF/LIF data, gross extrapolation or interpolation of data sets would have been necessary. Instead, the comparisons were made by integration of the PF/LIF data between the start and stop times of each data point of the compared method. The trapezoidal integration procedure employed gives a time-weighted average and linearly interpolates over periods of missing data. For the CAD/IC and FP/COL techniques, every data point was examined separately to determine if a sufficient number of PF/LIF data were present to allow a reasonable comparison to be made. In those cases with less than 50% coverage by PF/LIF data the DARE or MOADS results were used to determine trends in the ammonia levels. Only if the trends indicated that interpolation was appropriate was that point included. This procedure resulted in the deletion of 8 of 30 points from the FP/COL data and 12 of 38 points from the CAD/IC data. For the DARE and MOADS data sets all data with any overlap with PF/LIF data were retained.

One group of PF/LIF data was initially reported as approximately a factor of 10 lower than the results from the other techniques. After discussion between the investigator and the referee it was determined that an erroneous calibration constant had been used in the calculations. The corrected data were resubmitted and are included in all plots as diamonds.

In the following sections the results of the compared instrument will be plotted versus those from the PF/LIF technique, and linear regression fits will be extracted. The comparison plots will be presented on log-log plots to show more clearly the comparison over the full range of ammonia levels. However, note that the linear regression lines shown on these plots are curved if the intercept is nonzero. The results of the linear regressions are summarized in Table 5. In all cases the correlations are excellent; r^2 is 0.9 or better. However, the slopes and intercepts show some significant differences from unity and zero, respectively. The results of these regressions will be discussed below. The data sets from common inlet and separate inlets for the MOADS and DARE systems were significantly different and will be discussed separately. For the CAD/IC and FP/COL instruments the ambient data sets for both sampling modes will be discussed as a whole.

4.1. Comparison Between CAD/IC and PF/LIF

Figure 7 is a plot of ammonia as measured by the CAD/IC technique versus that from the PF/LIF technique for the total ambient air sampling period. One point is not on this plot because the ammonia level reported by the CAD/IC technique was 0 pptv. This data point is included in Figure 6, however, where it is plotted with a value of 1 pptv. It is likely that a problem with the blank occurred during this measurement. This data point has little influence on the linear regression fit. The slope indicates that CAD/IC yielded ambient measurements that were systematically lower, i.e., 85% of the PF/LIF results. However, this disagreement is within the combined estimated inaccuracies of the two techniques. No systematic dependence of the ratio of CAD/IC to PF/LIF results on relative humidity was found; this result is notable since the spiking tests that varied humidity were ambiguous for the CAD/IC technique. The ratio also did not depend on ambient temperature, ozone, NO_x , NO_y , CO, HNO_3 , or particulate ammonium or nitrate.

4.2. Comparison Between FP/COL and PF/LIF

Figure 8 shows the correlation between the FP/COL data and the PF/LIF data for the ambient sampling. The linear regression slope indicates that the FP/COL technique gave ammonia levels at about 66% of those from the PF/LIF method. The FP/COL data also can be directly compared with the CAD/IC results, since the exposure times of the two techniques were coincident. The linear regression of these two data sets is included in Table 5. The slope indicates that FP/COL gave results 80% of the CAD/IC values. The product of this percentage with the percentage from the section above (85%) agrees well with the 66% obtained from the regression of FP/COL with PF/LIF. The intercept is statistically not significantly different from zero, so there is no indication of a constant offset between any of these three techniques.

With respect to the low ammonia recoveries associated with the FP/COL method, the initial indication was that low ambient relative humidity was responsible for low filter collection efficiency. This FP/COL method was designed principally for use in the remote marine troposphere where low ammonia concentrations, moderate temperature, and high humidity are the predominant conditions. These are quite different from the ambient conditions during the majority of this instrument intercomparison. There was one period of high ($>70\%$) relative humidity, which occurred on March 20-21 (see Figure

TABLE 5. Results of Linear Regressions From the Instrument Result Comparisons for the Ambient Sampling

| Instrument | Slope | Intercept | r^2 | N |
|----------------------|-------|-----------|-------|------|
| CAD/IC versus PF/LIF | | | | |
| Total data set | 0.85 | -6 | 0.95 | 26 |
| FP/COL versus PF/LIF | | | | |
| Total data set | 0.66 | 159 | 0.94 | 22 |
| FP/COL versus CAD/IC | | | | |
| Total data set | 0.80 | -19 | 0.95 | 29 |
| MOADS versus PF/LIF | | | | |
| Common inlet | 0.84 | 111 | 0.99 | 132 |
| Separate inlet | 0.61 | 263 | 0.90 | 219 |
| | 0.63* | 165* | 0.92* | 178* |
| Total data set | 0.63 | 220 | 0.91 | 351 |
| | 0.64* | 177* | 0.94* | 310* |
| DARE versus PF/LIF | | | | |
| Common inlet | 1.24 | 123 | 0.90 | 30 |
| Separate inlet | 1.07 | 216 | 0.91 | 225 |
| | 1.06* | 264* | 0.90* | 191* |

The values for the intercepts are in parts per trillion by volume (pptv).

*Excluding data from episode of March 20 to 21 (see Figure 6).

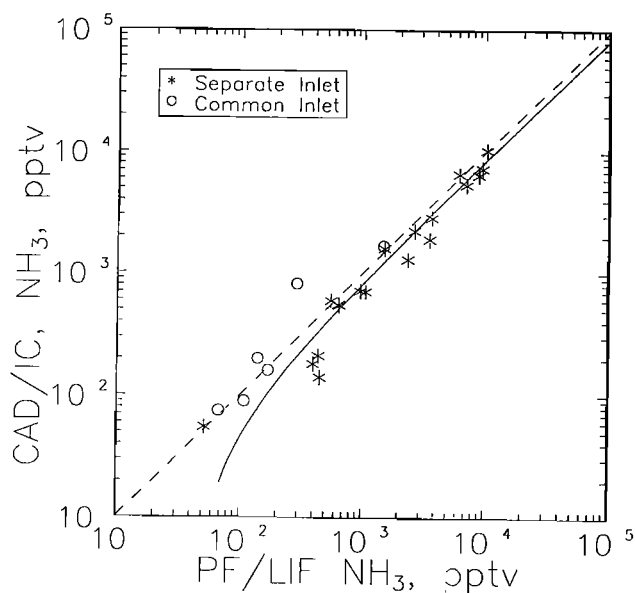


Fig. 7. Correlation between the ambient air data from the CAD/IC system and the corresponding PF/LIF data, which had been averaged over the integration times of the CAD/IC samples. The dashed line is that of one-to-one correspondence and the solid curve is the linear regression fit between the data sets. One CAD/IC data point at 0 pptv is not visible.

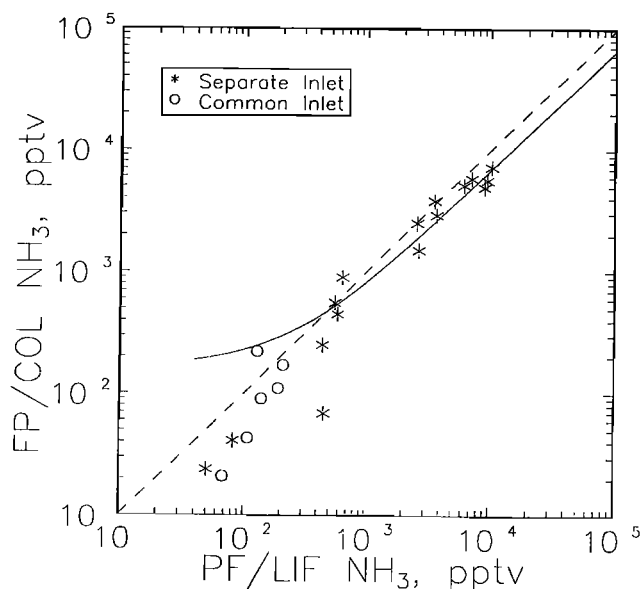


Fig. 8. Correlation between the ambient air data from the FP/COL system and the corresponding PF/LIF data, which had been averaged over the integration times of the FP/COL samples. The dashed line is that of one-to-one correspondence and the solid curve is the linear regression fit between the data sets.

6). The data points from this period are the three lowest separate inlet points in Figure 8. Under these conditions the FP/COL method still gave ammonia levels which were lower by about a factor of 2 from the PF/LIF data. This suggests that parameters other than relative humidity may influence the collection of ammonia by this method.

Of all the trace gas, particulate, and meteorological parameters measured, only temperature appears to correlate with changes in FP/COL ammonia recovery. Figure 9 shows the ratio of FP/COL to PF/LIF versus temperature for the entire ambient sampling period. Of the two outlying data points the one with the highest ratio is associated with a

FP/COL pump failure, but the other point is not associated with any unusual circumstances. Nevertheless, if the two outliers are neglected, then a significant correlation is observed (r^2 is 0.46). This suggests that recovery of gaseous ammonia by the FP/COL method is temperature dependent. However, low collection efficiency by the oxalic acid coated filters is probably not the principal cause of the low ammonia recoveries. This statement is supported by data from the individual filters, which can be used to calculate the collection efficiency for each individual ammonia measurement. These calculations show that in most cases the collection efficiency of the first filter in the pack was $\geq 90\%$, regardless of relative

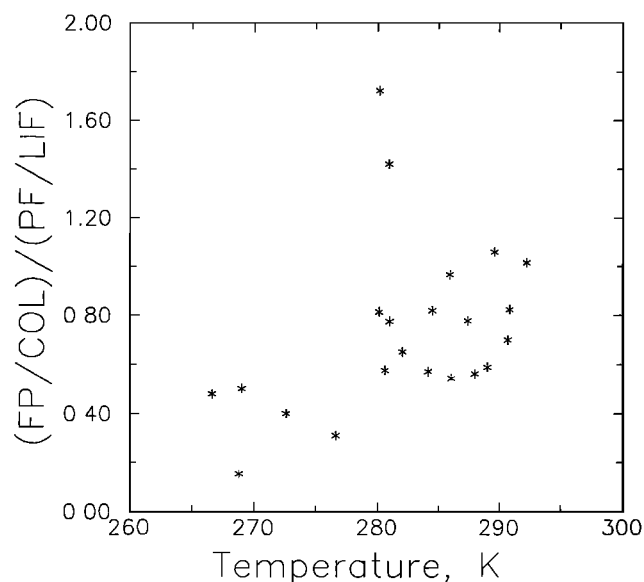


Fig. 9. Plot of the ratio of FP/COL to PF/LIF data versus the ambient temperature for all ambient sampling periods.

humidity. Moreover, low ammonia recovery from the extraction or analytical steps is unlikely since these occur under controlled conditions and have been shown to result in negligible losses [Quinn and Bates, 1989]. The most likely explanation for the low recoveries is loss of ammonia on either the filter holders or the Teflon prefilter, and it is not unreasonable to expect that this effect has a temperature dependence. Since measurements indicated that there was always sufficient ammonia to neutralize sulfuric acid, sorption of gaseous ammonia by acidic aerosol collected by the prefilter should be minimal. Loss of ammonia probably occurs directly on the material(s) involved, and the most likely material is the Teflon prefilter. Sorption of ammonia by Teflon has been noted in another study [Adema et al., 1990] and may have played a role in some results from the MOADS and DARE systems (see below). This effect was probably not noted in the laboratory study of the FP/COL method [Quinn and Bates, 1989] because all of the tests were conducted at temperatures greater than 20°C. The data in Figure 9 indicate that ammonia recovery should be complete at temperatures greater than this. The combination of high relative humidity and temperature never occurred during the course of this intercomparison, so an evaluation of this method under optimal conditions could not be made.

4.3. Comparison Between MOADS and PF/LIF

Figures 10 and 11 show the correlation between the MOADS data and the PF/LIF data for the separate and common inlet ambient air sampling periods, respectively. In Figure 10 the majority of the points at low ammonia levels is due to the fog episode during March 20 to 21 (described above). If the data from that period are deleted from the plot, then the intercept becomes significantly smaller but is still positive. The plot for the common inlet sampling period (Figure 11) shows a similar intercept, but the slope is closer to unity and there is a much higher correlation. For periods with mixing ratios below 1 ppbv the regression analysis gives a slope of 1.05 and an intercept of 80 pptv with $r^2 = 0.935$ and $N=82$. An earlier intercomparison between the MOADS and the CAD/IC techniques also showed higher measurements by the MOADS technique at low ammonia levels but a slope near unity for higher levels [Langford et al., 1989]. As noted earlier, degassing of adsorbed ammonia by the Teflon inlet

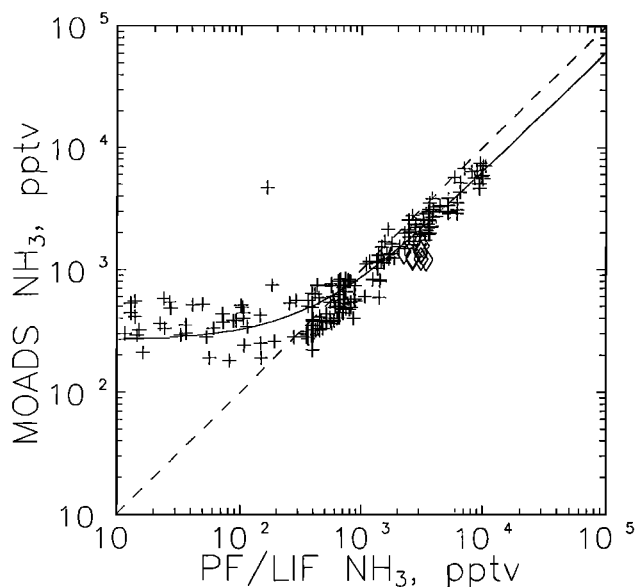


Fig. 10. Correlation between the separate inlet ambient air data from the MOADS system and the corresponding PF/LIF data, which have been averaged over the sample times of the MOADS instrument. The dashed line is that of one-to-one correspondence and the solid curve is the linear regression fit between the data sets. The diamond symbols are corrected PF/LIF data.

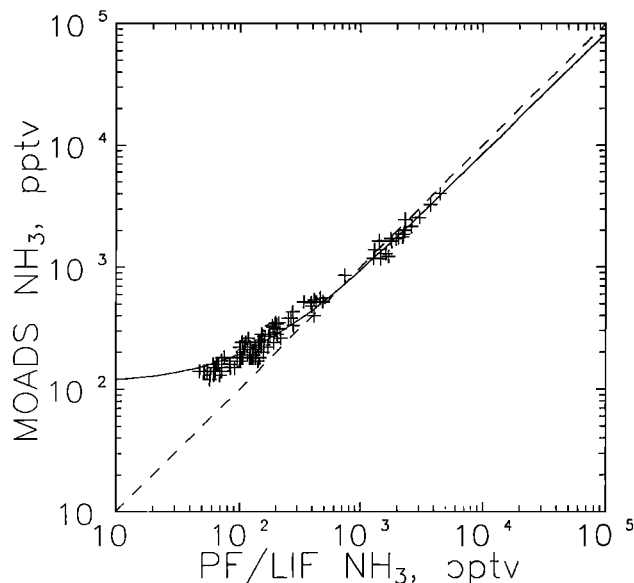


Fig. 11. Correlation between the common inlet ambient air data from the MOADS system and the corresponding PF/LIF data, which have been averaged over the sample times of the MOADS instrument. The dashed line is that of one-to-one fit between the data sets.

fitting may be responsible to some degree for the positive offsets seen in Figures 10 and 11.

Figures 10 and 11 differ significantly in both the slopes and the correlations. The better correlation in the common inlet data probably is due to sampling more homogeneous air parcels. Initially, no definitive explanation could be found for the significant (at the 95% confidence level) difference between the slopes for the two periods. When plotted for both

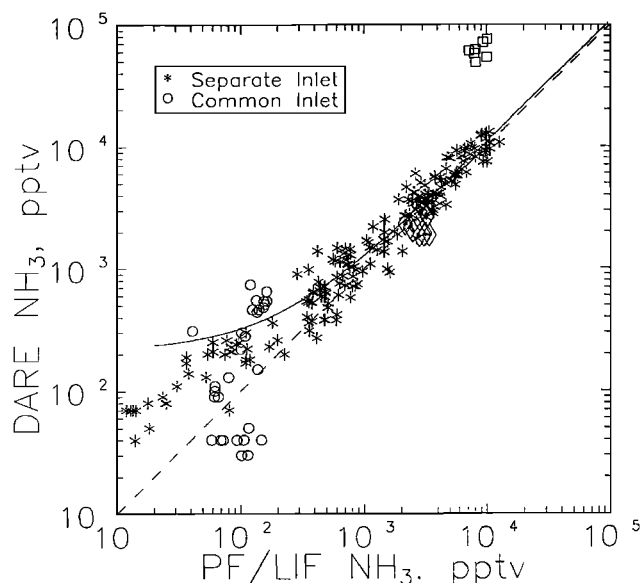
sampling periods (except for March 20–21), the ratio MOADS:PF/LIF does not systematically correlate with temperature, relative humidity, ozone, NO_x , NO_y , CO, or particulate ammonium. Furthermore, similar plots show no dependence on particulate nitrate or nitric acid for the separate inlet sampling period (no nitrate or nitric acid data were taken for the common inlet sampling period). On the other hand, the MOADS and PF/LIF data show reasonable consistency with respect to temporal variations in ammonia for most of the sampling times. A possible explanation of these effects is an error in calibration. As noted earlier the standards used by each instrument were independently evaluated and shown to be equivalent to within 10%, and the PF/LIF system agreed with the spike tests to within 6%. Thus if ammonia calibration problems are responsible for the difference between the instruments, then it is likely due to the MOADS system. After the MOADS data were turned in, an extensive analysis by the MOADS principal investigator indicated that the difference between the slopes in Figures 10 and 11 could have been due to a change in the NO internal standard used to normalize the temperature-dependent response of the chemiluminescence detector. An unexplained 35% decrease in the NO internal standard signal level between March 27 and April 7 (possibly due to a malfunction of the NO standard mass flow controller or gas tank regulator) was not noticed at that time. Since the calibration curve used to analyze the separate inlet data of March 20–27 was generated on March 29, the NO detector response may have been only $\approx 68\%$ of the assumed level. Consequently, the calculated NH_3 mixing ratios may have been similarly underestimated. If this effect is assumed to be responsible for incorrect MOADS separate inlet data, then substantially better agreement would be seen between the PF/LIF and corrected MOADS data sets (regression slope, 1.02; intercept, 18 pptv). However, whether or not the above analysis is correct, the fact remains that the data acquired during the intercomparison show deficiencies in the MOADS system that will need to be addressed in the future.

In summary, plots of data from the intercomparison show that compared to the PF/LIF system, the MOADS instrument underestimated ammonia at higher mixing ratios and overestimated ammonia at lower mixing ratios. As noted above, these effects may be due to calibration problems and, to some extent, degassing of adsorbed ammonia by the Teflon inlet fittings. For this analysis, though, it seems reasonable to treat the common inlet and free sampling data sets together and exclude the March 20 to 21 data to get the best comparison of the MOADS system to the PF/LIF system, shown in Table 5.

4.4. Comparison Between DARE and PF/LIF

Figure 12 shows the correlation between the DARE data and the PF/LIF data for the ambient air sampling period. Again, the diamond symbols represent corrected PF/LIF data. The square symbols on this plot denote data from the DARE instrument that were submitted but labeled as uncertain due to a system carrier gas problem; these data were not included in the linear regressions of Table 5. However, it is apparent from examination of a plot of ammonia versus time (not shown) that these points follow the same trend as the PF/LIF data but are offset to higher values. This is consistent with the systematic problem described above. One final note regarding Figure 12 concerns the DARE common inlet data cluster at 500 pptv. The DARE instrument principal investigator reported RF interference during this period, so these data may have greater uncertainty than the rest of the common inlet data points.

The very different appearance between the data sets from the two ambient sampling periods indicates a major difference in the operation of the DARE instrument between the two sampling modes. The higher degree of scatter at low levels in the common inlet data set suggests that there was a problem when the DARE instrument sampled through the common



12. Correlation between the ambient air data from the DARE system and the corresponding PF/LIF data, which have been averaged over the sample times of the DARE instrument. The dashed line is that of one-to-one correspondence and the solid curve is the linear regression fit between the data sets. The diamond symbols are corrected PF/LIF data. The squares are uncertain DARE data which have not been included in the linear regression.

inlet. This observation is consistent with the discussion of the spike test data (see above). The principal change for the DARE technique between the two sampling modes was in the inlet configuration. While sampling from the common manifold, the inlet line included a Teflon-lined flexible stainless steel length of tubing, but when the DARE instrument was configured for separate inlet sampling, this piece was removed. It is possible that this tubing was responsible, via some type of surface effect or leak, for the scatter observed in the DARE data from the spike tests and the common inlet sampling period. This scatter is not manifest in the linear regression analysis for the entire common inlet sampling period (Table 5) since the fit is dominated by the one point at 3 ppbv. On the other hand, as noted earlier, the DARE and PF/LIF data from the March 14–15 common inlet sampling period show very good agreement on average but somewhat less agreement temporally (see Figure 5).

For the separate inlet data at high levels the DARE system agrees very well with the PF/LIF system. This is especially apparent from how well these systems track variations in ammonia level over time. If the relationship between the DARE and PF/LIF data were linear, the 216 pptv intercept from the linear regression would suggest serious disagreement at low levels. However, the separate inlet data in Figure 12 show an offset of only about 50 to 100 pptv between the DARE and PF/LIF data at the lowest ambient levels, so the relationship between the two data sets is not exactly linear. Most of these low ammonia values occurred during the period of fog and low temperatures on March 20–21 when the largest fractional difference between the DARE and PF/LIF systems was observed. If these data are excluded, the slope of the regression line does not change significantly but the intercept increases to 264 pptv. The intercepts from the linear regression analyses are determined primarily by the data between 0.5 and 1.0 ppbv, which do show offsets of the order of the intercept. Although the high intercepts seem to indicate a potential positive interference in the DARE system, no systematic trends

were seen in plots of the ratio DARE:PF/LIF versus particulate ammonium and nitrate or gaseous species such as nitric acid, NO_x, ozone, and CO. Finally, a previous report [Appel et al., 1988] has shown a temperature dependence of the ratio of results from a tungsten acid denuder system to those of an FTIR spectroscopic technique. In this study no such relationship was found in plots of the ratio DARE:PF/LIF with temperature, relative humidity, or other meteorological factors.

5. Summary and Conclusions

Two of the techniques, the PF/LIF and the CAD/IC methods, measured approximately 90% of the calculated ammonia added in the spiking tests and agreed very well with each other in the ambient measurements. Considering that some of the added ammonia may have been lost in the manifold before sampling by these techniques, their performance in the spiking tests is consistent with 100% detection efficiency. In the ambient measurements the linear regression between the two data sets indicated that the CAD/IC measured about 85% of the PF/LIF values, which is well within their combined uncertainties. Thus the tests performed in this intercomparison indicate that both of these techniques are fully capable of measuring ammonia in the troposphere. Operationally, the PF/LIF technique was capable of accurately following changes in ammonia levels over short time intervals (1 min). With respect to the deployment and operation of this instrument there are some disadvantages: While the system is automated, it cannot run unattended for long periods of time because the lasers need constant attention, it is technically complex and uses corrosive chemicals, and it requires large amounts of electrical power. On the other hand, with some modifications, this instrument can be configured for use on an aircraft. Sample acquisition times for the CAD/IC technique are typically 2 hours, so fine time resolution is not possible. While this method is very labor intensive and cannot be automated easily, equipment requirements (and costs) are modest.

The ambient air data show that the FP/COL method measured about 66% of the ammonia, as determined by the PF/LIF technique, and the ammonia spiking tests indicated even lower fractional determinations. Previous tests [Quinn and Bates, 1989] have shown that collection efficiencies of oxalic acid coated filters are near 100% at 75% relative humidity and 20°C, and data from individual filters for these ammonia determinations indicate that the collection efficiency of the first filter generally was $\geq 90\%$, regardless of humidity and temperature. Under the conditions of this study the low FP/COL ammonia recovery values appear to be due more to the temperature-related loss of ammonia on the Teflon prefilter and/or the filter holders than to inefficient filter collection. Thus it is likely that deployment of the FP/COL method under conditions similar to this intercomparison, principally low ambient temperature, will adversely affect the filter pack ammonia determinations. This system requires sample times of the order of 2 hours or longer and is somewhat labor intensive. On the other hand, the system is reasonably portable and equipment costs are modest.

The MOADS data from the combined ambient air sampling periods were highly correlated ($r^2 = 0.920$) with the PF/LIF data, but the linear regression slope indicated that this technique detects 64% of the ammonia that is observed by the PF/LIF method for levels greater than about 1 ppbv. Below this level there is a tendency for MOADS to overestimate ammonia, which may be related to sorption and subsequent outgassing of ammonia by the Teflon inlet fitting. For the common inlet period the MOADS data were 84% of the PF/LIF data for levels above 1 ppbv and 105% for ammonia less than 1 ppbv. No satisfactory explanation for the discrepancy between the common inlet and separate inlet sampling periods was apparent from the spike test results or

from ancillary data acquired during the ambient sampling periods. However, as discussed in a previous section, these differences may be attributable to a problem with the MOADS calibration and suggest that the calibration procedure should be improved. Other phenomena may also contribute to the observed differences. With respect to deployment the MOADS system is automated, samples every 30 min, and is capable of unattended operation for up to 7 days.

The DARE technique showed very good agreement with the PF/LIF method for the period of ambient sampling with separate inlets. The linear regression indicated a DARE versus PF/LIF slope of 1.07 with a constant offset (DARE above PF/LIF) of 216 pptv indicated by the intercept. However, the lowest separate inlet ammonia measurements show an offset of only 50 to 100 pptv. Analysis of a specific 24-hour period of common inlet sampling indicated that the DARE and PF/LIF systems agreed, on average, to within about 30% at low ammonia levels (100 pptv), but these same data did not correlate well temporally. The DARE data from the common inlet and spike tests may have been influenced by the transfer line that contained a section of Teflon-lined flexible stainless steel tubing. The DARE system is automated, is capable of sampling every 10-15 min, and can be flown on aircraft.

The spike tests of potential interferants did not definitely identify any interferences in any of the methods. However, the upper limits that could be placed on potential interferences often were not very stringent. Results of particular note include the PF/LIF technique accommodated large changes in relative humidity with no apparent loss of accuracy even though water vapor quenching reduces the fluorescence that the instrument monitors [van Dijk et al., 1989]. There was some indication of a positive interference by methylamine in the MOADS system, but more tests would be required to definitely establish this.

Evidence from the ambient air data for March 20-21 (Figure 6) indicates that the formation of fog causes ambient ammonia to be primarily partitioned into the condensed phase, leaving the interstitial air greatly depleted. The MOADS system, with its inlet and sampling system at 50°C, overestimated the gaseous ammonia mixing ratio by as much as a factor of 40 compared to the PF/LIF results. This may result from the small (≤ 0.5 mm) annular spacing of the MOADS denuders and the heating of the inlets and denuders to 50°C during sampling. Thus it is likely that the MOADS system gave a measurement of total ammonia as a result of volatilization of absorbed ammonia from water droplets or ice crystals entrained in the sampled air, while the PF/LIF system measured only gas phase ammonia as a result of very fast sample flow and operation at ambient sample temperatures.

In general, the intercomparison results indicate that the reliability of data from any ammonia detection system may well depend on the specific configuration of the instrument inlet system and the conditions under which it is operated. Moreover, these observations suggest that the use of Teflon components of even short length should be avoided in the measurement of ammonia.

Acknowledgements. The authors thank Paul Murphy for the data reduction software and support in the interchange of data and Ken Aiken for assistance in the field operations. This research was supported by the National Oceanic and Atmospheric Administration as a part of the National Acid Precipitation Assessment Program.

References

- Adema, E. H., J. R. Ybema, P. Heeres, and C. P. Wegh, The heterogeneous formation of N₂O in air containing NO₂, O₃, and NH₃, *J. Atmos. Chem.*, **11**, 255-269, 1990.

- Appel, B. R., Y. Tokiwa, E. L. Kothny, R. Wu, and V. Povard, Evaluation of procedures for measuring atmospheric nitric acid and ammonia, *Atmos. Environ.*, **22**, 1565-1573, 1988.
- Braman, R. S., T. J. Shelley, and W. A. McClenny, Tungstic acid for preconcentration and determination of gaseous and particulate ammonia and nitric acid in ambient air, *Anal. Chem.*, **54**, 358-364, 1982.
- Braman, R. S., M. A. de la Cantera, and Q. X. Han, Sequential selective hollow tube preconcentration and chemiluminescence analysis system for nitrogen oxide compounds in air, *Anal. Chem.*, **58**, 1537-1541, 1986.
- Fahrquar, G. D., R. Wetselaar, and B. Weir, Gaseous nitrogen losses from plants, in *Gaseous Loss of Nitrogen From Plant-Soil Systems*, edited by J. R. Freney and J. R. Simpson, Martinus Nijhoff/W. Junk, The Hague, 1983.
- Ferm, M., Method for determination of atmospheric ammonia, *Atmos. Environ.*, **13**, 1385-1393, 1979.
- Ferm, M., H. Areskoug, J.-E. Hanssen, G. Hilbert, and H. Lattila, Field intercomparison of measurement techniques for total NH_4^+ and total NO_3^- in ambient air, *Atmos. Environ.*, **22**, 2275-2281, 1988.
- Finlayson-Pitts, B. J., and J.N. Pitts, Jr., *Atmos. Chem.*, John Wiley, New York, 1986.
- Gras, J. L., A field comparison of two atmospheric ammonia sampling techniques, *Tellus*, **36(B)**, 38-43, 1984.
- Harrison, R. M., and A.-M. N. Kitto, Field intercomparison of filter pack and denuder sampling methods for reactive gaseous and particulate pollutants, *Atmos. Environ.*, **24(A)**, 2633-2640, 1990.
- Harwood, J. E., and A. L. Kuhn, A colorimetric method for ammonia in natural waters, *Water Res.*, **4**, 805-811, 1970.
- Langford, A. O., P. D. Goldan, and F. C. Fehsenfeld, A molybdenum oxide annular denuder system for gas phase ambient ammonia measurements, *J. Atmos. Chem.*, **8**, 359-376, 1989.
- LeBel, P. J., J. M. Hoell, J. S. Levine, and S. A. Vay, Aircraft measurements of ammonia and nitric acid in the lower troposphere, *Geophys. Res. Lett.*, **12**, 401-404, 1985.
- LeBel, P. J., B. J. Huebert, H. I. Schiff, S. A. Vay, S. E. VanBramer, and D. R. Hastie, Measurements of tropospheric nitric acid over the western United States and northeastern Pacific Ocean, *J. Geophys. Res.*, **95**, 10,199-10,204, 1990.
- LeBel, P. J., S. A. Vay, and P. D. Roberts, Ammonia and nitric acid emissions from wetlands and boreal forest fires, in *Global Biomass Burning Atmospheric, Climatic, and Biospheric Implications*, edited by J. S. Levine, pp. 225-229, MIT Press, Cambridge, Mass., 1991.
- Lobert, J. M., D. H. Scharffe, T. A. Kuhlbusch, R. Seuwen, W. M. Hao, and P. J. Crutzen, Biomass burning as a source of atmospheric nitrogen containing compounds: An experimental study, in *Abstracts of the Seventh International Symposium of the CACGP*, p.135, Chamrousse, France, 1990.
- National Atmospheric Deposition Program, *NADP/NTN Annual Data Summary: Precipitation Chemistry in the United States, 1989*, Nat. Resour. Ecol. Lab., Ft. Collins, Colo., 1989.
- National Research Council (NRC), Subcommittee on ammonia, *Ammonia*, Washington, D.C., 1979.
- Quinn, P. K., and T. S. Bates, Collection efficiencies of a tandem sampling system for atmospheric aerosol particles and gaseous ammonia and sulfur dioxide, *Environ. Sci. Technol.*, **23**, 736-739, 1989.
- Roberts, J. M., A. O. Langford, P. D. Goldan, and F. C. Fehsenfeld, Ammonia measurements at Niwot Ridge, Colorado, and Point Arena, California, using the tungsten oxide denuder tube technique, *J. Atmos. Chem.*, **7**, 137-152, 1988.
- Schendel, J. S., R. E. Stickel, C. A. van Dijk, S. T. Sandholm, D. D. Davis, and J. D. Bradshaw, Atmospheric ammonia measurement using a VUV/photofragmentation laser-induced fluorescence technique, *Appl. Opt.*, **29**, 4924-4937, 1990.
- Seinfeld, J. H., *Atmospheric Chemistry and Physics of Air Pollution*, John Wiley, New York, 1986.
- Sickles, J. E., II, L. L. Hodson, E. E. Rickman, Jr., M. L. Saeger, D. L. Hardison, A. R. Turner, C. K. Sokol, E. D. Estes, and R. J. Paur, Comparison of annular denuder system and the transition flow reactor for measurements of selected dry deposition species, *JAPCA*, **39**, 1218-1224, 1988.
- Solarzano, L., Determination of ammonia in natural waters by the phenylhypochlorite method, *Limnol. Oceanogr.*, **14**, 799-801, 1969.
- Torres, A. L., Nitric oxide measurements at a nonurban eastern United States site: Wallops instrument results from July 1983, GTE/CITE mission, *J. Geophys. Res.*, **90**, 12,875-12,880, 1985.
- van Dijk, C. A., S. T. Sandholm, D. D. Davis, and J. D. Bradshaw, $\text{NH}(b^1\Sigma^+)$ deactivation/reaction rate constants for the collisional gases H_2 , CH_4 , C_2H_6 , Ar, N_2 , O_2 , H_2O , and CO_2 , *J. Phys. Chem.*, **93**, 6363-6367, 1989.
- Wallace, J., and P. V. Hobbs, *Atmospheric Science. An Introductory Survey*, Academic, San Diego, Calif., 1977.
- Warneck, P., *Chemistry of the Natural Atmosphere*, Academic, San Diego, Calif., 1988.
- Wiebe, H. A., et al., A comparison of measurements of atmospheric ammonia by filter packs, transition-flow reactors, simple and annular denuders and Fourier transform infrared spectroscopy, *Atmos. Environ.*, **24(A)**, 1019-1028, 1990.
- J. D. Bradshaw, S. T. Sandholm, and J. S. Schendel, School of Earth and Atmospheric Sciences, Georgia Institute of Technology, Atlanta, GA 30332.
- M. P. Buhr, F. C. Fehsenfeld, A. O. Langford, R. B. Norton, D. D. Parrish, B. A. Watkins, and E. J. Williams, Aeronomy Laboratory, National Oceanic and Atmospheric Administration, 325 Broadway, Boulder, CO 80303.
- J. G. Calvert, National Center for Atmospheric Research, 1850 Table Mesa Drive, Boulder, CO 80307.
- P. J. LeBel and S. A. Vay, Langley Research Center, National Aeronautics and Space Administration, Hampton, VA 23665.
- P. K. Quinn, Pacific Marine Environmental Laboratory, National Oceanic and Atmospheric Administration, 7600 Sand Point Way Northeast, Seattle, WA 98115.
- P. D. Roberts, College of William and Mary, Williamsburg, VA 23186.

(Received May 6, 1991;
revised March 24, 1992;
accepted March 24, 1992.)